Building isotype-optimized pathogen-specific mAbs from memory B cells

Malika Hale

A dissertation

submitted in partial fulfillment of the

requirements for the degree of

Doctor of Philosophy

University of Washington

2023

Reading Committee:

David Rawlings, Chair

Marion Pepper

W. Conrad Liles

Program Authorized to Offer Degree:

Molecular and Cellular Biology

University of Washington

Abstract

Building isotype-optimized pathogen-specific mAbs from memory B cells

Malika Hale

Chair of the Supervisory Committee:

Professor David J. Rawlings

Seattle Children's Research Institute

Department of Pediatrics

Emerging viruses and antibiotic-resistant bacteria are major threats to human health. Despite well-established benefits of the passive transfer of immunity in animal models, engineered monoclonal antibodies (mAbs) have struggled to achieve consistently positive results for the treatment of infectious disease in humans. We hypothesized that a strategy of building mAbs based on human immune memory B cells (MBCs) could be advantageous. This thesis describes efforts to develop mAbs with plausible therapeutic potential against two microbes that drive severe morbidity in vulnerable patients: *Pseudomonas aeruginosa* and SARS-CoV-2. Diverging from historical, animal-based methods for mAb discovery, we used the B cell receptor sequences of human, antigen-specific B cells, with special focus on MBCs, as templates for novel mAbs.

Focusing first on *P. aeruginosa*, we generated anti-bacterial mAbs using source B cells obtained from patients seen at a cystic fibrosis (CF) clinic. CF is a genetic condition associated with unusually frequent *P. aeruginosa* infections, but not defects in adaptive immunity. In an *in vivo* pneumonia model with a highly virulent strain, 2 of 2 human-derived mAbs exhibited prominent protective activity. Notably, our new mAbs were noninferior to an extensively engineered mAb that comprises half of the bi-specific clinical candidate, gremubamab. A second panel of MBC-derived mAbs that showed promise *in vitro* remain to be tested in future work, highlighting the efficiency of our mAb discovery strategy. Further, we believe our study contributes to understanding of immunity in CF, being the first to confirm the presence of *P. aeruginosa*-specific MBCs in CF patients.

In contrast to *P. aeruginosa*, mAbs targeting SARS-CoV-2 were developed from human B cells contemporaneously by multiple groups including our team. However, circulating escape variants have significantly limited clinical use. Importantly, consistent with nearly all mAbs in clinical use, these vulnerable mAbs were of the monomeric isotype, IgG. Building on our prior studies of MBCs and evidence that an alternative isotype, IgM, was an important component in virus-neutralizing human serum, we cloned new mAbs from SARS-CoV-2-specific IgM MBCs. We also found that diverse MBC-derived mAbs gained greater neutralizing potency when expressed as the naturally pentameric IgM isotype. Importantly, we showed that IgM mAbs retained neutralizing activity against viral variants that evaded otherwise identical mAbs made in the IgG isotype. These results suggest a biological role for IgM MBCs in protection against rapidly mutating pathogens, and illuminate the potential for IgM mAbs in the search for new treatments for infectious diseases.

TABLE OF CONTENTS

LIST OF FIGURES

LIST OF TABLES

ACKNOWLEDGEMENTS

I would like to express my deepest gratitude to my mentor, the wholly incomparable Dr. David J. Rawlings. To be a graduate student in the Rawlings lab is to climb with perfect trust in your belayer. I also thank Dr. Marion Pepper, who acted as a co-mentor and second source of leadership, vision and support. This work benefited from the guidance of an exceptional Committee, Drs. Jason Debley, Justin Kollman, W. Conrad Liles, and Erick Matsen. Reading committee members reviewed this work on a challenging timeline at the busiest time in an overfull year. Thank you.

I thank Jennifer Haddock for indispensable assistance. I would also like to acknowledge the contributions to my scientific training, before and during graduate school, of more than a hundred current and former members of the Rawlings lab and its close affiliates. For the work included in this dissertation, particular acknowledgement is due to Rawlings lab scientists Christopher Thouvenel and Drs. Yu Chen and Andrea Repele, and to Drs. Jason Netland and Lauren Rodda of the Pepper lab. The paths clinical samples traveled to reach my lab bench were cut and maintained by physician scientists and research nurses at Seattle Children's and the University of Washington. I am grateful to them and to the many strangers who gave their B cells for our research.

For good advice, intellectual input, and personal support, I am deeply grateful to my friends, including my generous ARCS donors, Sandy & Kent Carlson and Drs. Luciana Simoncini & Todd Scheuer, my E-18 classmates in the University of Washington Medical Scientist Training Program, and the inimitable Dr. Karen Sommer. In all I do, I am significantly advantaged by the love and inspiration of the best and bravest parents, sister, grandmothers, aunts, and uncles. Finally, I would like to acknowledge Drs. Mary Claire King and Marshall S. Horwitz, whose early belief and fierce support brought me home to the Rawlings lab.

DEDICATION

In memory of Sunil,

who taught me to ride a bicycle,

and for David and Karen,

who led the way on the climbs.

Chapter 1. Introduction

Encounters with adapting and emerging respiratory pathogens are inevitable in human life. Thanks to our remarkable immune system, most individuals can expect to emerge from infectious confrontations without suffering severe illness. Vaccines and antimicrobial drugs are critical tools to further limit morbidity, especially for vulnerable individuals. Prior to the advent of SARS-CoV-2, respiratory infections were already a leading cause of death locally and globally (1). The novel coronavirus pandemic brought significant public attention to the morbidity and mortality of infectious disease in the absence of effective treatments, as well as the benefits and challenges of employing antibody therapies to fill the gap. As further illustrated by the toll of antibiotic-resistant bacterial pneumonias (2,3), additional treatment options are needed for long-standing pathogens as well as newly emerging threats.

1.1 ANTIBODIES

Antibodies, the central component of humoral immunity, are secreted glycoproteins that bind to their target antigens with exquisite specificity. Diverse, antigen-specific antibodies are produced in vertebrates by terminally differentiated descendants of the B cell lineage as part of an adaptive immune response (4,5). *Ex vivo*, an antibody whose protein/nucleotide sequence and binding target are known can be produced as a monoclonal antibody (mAb) for use in medicine or research (6).

A monomeric antibody is roughly a Y shape, with each arm of the Y made of paired heavy- and light chains. The interface of heavy and light chain variable regions forms an N terminal binding pocket (paratope) that determines target specificity. Within the variable regions, the length

and composition of hypervariable loops within the antigen-binding site (complementary determining regions, CDRs) have particular influence on binding specificity (6). Antibody stalks (Fc), composed of heavy chain constant regions, do not contribute significantly to specificity, but instead provide effector functions, tolerant scaffolding, and quaternary structure.

In nature, a limited number of constant region sequences are employed. Light chain constant regions are either kappa or lambda, without functional distinction. Mu, gamma, alpha, epsilon, and delta heavy chain constant regions define immunoglobulin (Ig) isotypes, respectively IgM, IgG, IgA IgE and IgD. IgG and IgM predominate in serum (7,8), and are of the greatest relevance to this work. IgG is a monomer whether expressed on the surface as membrane-bound Ig or secreted as an antibody. In contrast, only surface IgM is a monomer. When the transmembrane domain is spliced out in antibody-secreting cells, IgM self-assembles as a pentamer in the presence of joining (J) chain protein (9). The pentameric structure has important functional consequences. Binding sites for complement proteins are present within the Fcs of IgM and IgG. Complement-opsonized IgG and IgM immune complexes are taken up by antigen-presenting cells, including migrating follicular B cells that facilitate antigen delivery to lymph nodes (10). However, the flexed, pentameric structure of antigen-bound IgM facilitates more rapid activation of C1q, which is also a pentamer (9); in contrast, multiple IgG Fc must complex together to achieve similar activation (11).

Fc receptors (FcRs) are expressed by immune and non-immune cells, mediating effector functions and physiologic distribution. For example, renal epithelial cells express FcRn, which facilitates re-uptake of filtered IgG antibody, extending the serum half-life of IgG (12). Meanwhile, natural killer cells express FcγRIIIB which enables recognition of IgG antibodies bound to an infected cell, triggering antibody-dependent cytotoxicity (ADCC) (3). Human

therapeutic mAbs also perform effector functions *in vivo*. In fact, single nucleotide polymorphisms in FcRs that alter antibody binding affinity impact the clinical efficacy of anti-tumor mAbs that rely on ADCC (13,14). In addition to performing effector functions, pathogen-bound antibodies may directly block (neutralize) infection or pathogenesis via steric hindrance or forced conformational change at critical site(s) (15). Neutralizing activity depends on an antibody's target epitope, affinity, and avidity. Pathogen-specific factors include its mechanism of infection and immune evasion strategies, and the density and accessibility of the antibody's target are equally important. Protective antibodies may prevent infection by binding to a pathogen, eg. by blocking a viral docking protein to prohibit interaction with host cells. However, even non-neutralizing antibodies can confer protection *in vivo* via effector functions, accelerating an immune response as a central node that connects adaptive immunity to other branches of the immune system.

1.2 Antibodies as Therapeutic Agents For Treatment of infectious diseases

The first understanding of antibodies emerged from experiments in which serum transferred from pathogen-exposed animals conferred immediate protection to their naïve siblings (8). Early attempts to use antibody-based therapies in human medicine also began with infectious diseases (8,16). However, in the modern era, most clinical mAbs are used for the treatment of noncommunicative illness (*eg.* autoimmunity, cancer, familial hypercholesterolemia), and only a handful are used in the treatment of infectious diseases (17). Of the anti-infectious mAbs now approved in the US, three bind to secreted bacterial toxins: obiltoxaximab and raxibacumab (anti-anthrax toxin (18)) and bezlotuximab (anti-toxin B for prevention of *Clostridioides difficile* recurrence (17)). Two are neutralizing antibodies that bind to viral glycoproteins: ansuvimab (anti-

Ebolavirus (19,20)) and palivizumab (anti-respiratory syncytial virus (21)). One blocks infection by binding a T cell surface receptor (CD4) used by human immunodeficiency virus (HIV): ibalizumab (22). There is significantly more clinical experience, and thus data, available for mAbs targeting cancer and autoimmune disease. Therefore, this text describes some lessons learned from the use of non-pathogen-directed mAbs that are likely also to apply to mAbs used to treat infectious disease. Where possible, an example of an analogous infectious disease mAb is also noted.

1.3 HYBRIDOMAS

Most commercial mAbs today are derivations of an antibody that was once produced *in vivo* by a murine plasmablast in response to a recombinant protein and adjuvant (17). For example, development of the now commonly prescribed anti-TNF therapeutic mAb, infliximab (23), began three decades ago with five intraperitoneal injections of recombinant TNF, with and then without Freund's adjuvant, into an immune-competent mouse (24). Following immunization, clonal, antibody-secreting hybridomas were made by fusing serially diluted lymphocytes with an immortal cell line. Supernatants collected from individual hybridoma cultures were screened for binding to the recombinant protein. Promising clones were then expanded in cell culture and sequenced. Similar methods were used more recently to develop the three component mAbs in a cocktail tested clinically to treat Ebola (25,26). Although the process of obtaining antibody sequences from the select, clonally-expanded cells has been dramatically streamlined by technological advances in the last 30 years (27), murine hybridomas remain the most common source cells for clinical mAbs (28), using methods for their generation otherwise little changed since 1993 (24,29).

1.4 ANTIBODY DISCOVERY, IMMUNOGENICITY AND HUMANIZATION

A variety of approaches have been employed to reduce the immunogenicity of animal-derived mAbs intended for use in humans. Cross-species anti-immunoglobulin immune reactions were well-appreciated a century ago, when it was observed that immunized horse serum (then in clinical use as diphtheria anti-toxin), caused dramatic, febrile illness more severe than if unimmunized horse serum was given (16). Rarely, serum-sickness-like reactions are reported for clinical mAbs that retain some murine sequence (30). More commonly, immune responses are tolerated until the resulting anti-drug antibodies neutralize therapeutic effect (31,32).

In the case of infliximab (24) and the experimental anti-Ebolavirus cocktail (26), the specificity-determining variable (V) regions of the parent hybridoma were taken *en bloc* for linkage to human constant regions, resulting in antibodies that are ~70% human. For other commercial mAbs, immunogenicity was further reduced by partial humanization of the V regions. This approach was used for palivizumab (anti-respiratory syncytial virus (33)), and many anti-cancer mAbs, *eg.* pembrolizumab (anti-PD-1 (34)) (33,35). Overall, 49 of 79 FDA-approved antibody products in 2020 were humanized or chimeric mAbs derived from animal hybridomas (17). Despite efforts at humanization, anti-drug antibodies that neutralize biologic medicines remain clinically significant, especially for patients being treated for chronic diseases (31,36). Avoidance of immunogenicity will be equally important for the success of antimicrobial antibodies, where long-term use might be desirable as infectious prophylaxis in high-risk patients.

1.5 ANTIBODY DISCOVERY IN HUMAN MIMETIC SYSTEMS

Several novel systems have been established to generate “fully human” mAbs. For example, hybridomas can be generated using immune-competent mice that are transgenic for

human variable regions (33). The resultant clinically approved mAbs are promoted as enhanced, second-generation iterations of existing mAbs, *eg.* ofatumumab (anti-CD20 (37), compare to rituximab) and golimumab (anti-TNF (38), compare to infliximab). An experimental anti-pseudomonal clinical candidate bispecific, gremubamab, incorporates an antibody that was developed using similar methods (39). Perhaps the best known mAb product, a component of the Regeneron cocktail approved for emergency use during the COVID-19 pandemic, casivirimab, was identified using Regeneron's exclusive strain of human-transgenic mice (40). This method is relatively slow and costly; breeding pairs sufficient to start a colony have been reported to cost more than a hundred million dollars (33) and such strains are not generally available to most researchers.

An alternative method that is much more broadly accessible, phage display libraries are used for high-throughput screening via random assembly of human heavy (VH) and light (VL) chain variable regions *in vitro* (41). Affinity optimization can be performed by introducing random mutations and re-testing selected candidates (39). Advantages of this approach include its speed and that it can be readily used to generate antibodies against highly conserved targets. This approach, however, lacks key events provided by the adaptive immune system *in vivo*, including germinal center-mediated affinity maturation and negative selection. Examples of clinical mAbs produced using phage display include adalimumab (anti-TNF (42,43)) and belimumab (anti-BAFF (44,45); approved for use in lupus nephritis). Among many variations on phage display, one interesting approach that uses a single, tolerant scaffold VH and varies only the complementary determining regions (CDRs) has been used to produce experimental antibodies, although none have been tested in humans (46). A few anti-SARS-CoV-2 mAbs that received temporary

authorization for COVID-19 were identified using phage display wherein VH/VL libraries were generated from peripheral blood cells of previously-infected individuals (47).

Rigorous comparisons of mAbs derived by different methods are not feasible in human clinical studies. However, clinical trials using anti-TNF mAbs provide insight regarding the effect of antibody sequences on immunogenicity. Anti-drug antibodies against the TNF inhibitor mAbs are known neutralize therapeutic effect and are therefore closely tracked in clinical trials. Patients treated with infliximab (mouse-human chimera (24)) do indeed appear more likely to develop anti-drug antibodies than those treated with adalimumab (human VH phage display (42)) or golimumab (hybridoma from mice with human V genes (38)) (36). Golimumab is associated with the lowest rates of anti-drug antibodies. Results in TNF inhibitors in autoimmune disease may not be more broadly generalizable, and a single mAb in each source category limits interpretation further. Nevertheless, available data supports the hypothesis that fully human mAbs may outperform mAbs with residual xenogeneic features in real-world clinical use.

1.6 HUMAN MEMORY B CELLS

The adaptive immune system generates a vast array of highly-specific, protective antibodies in response to diverse pathogens throughout our lifetime. In designing anti-infectious mAbs, it may be beneficial to consider the larger context in which effective endogenous antibody structures are produced, selected and maintained. Unlike plasma cells, MBCs are not antibody-secreting, instead expressing heavy- and light-chains as membrane-bound immunoglobulin, a component of the B cell receptor (BCR) (48). Re-encounter with the cognate antigen triggers BCR signaling, activation, and differentiation into antibody-secreting cells (5). Consequently, the BCR

repertoire of MBCs may be considered as a living library that is enriched for pathogen-specific sequences.

In a classical germinal center (GC) immune response, long-lived memory B cells (MBCs) arise in parallel with long-lived antibody-secreting plasma cells (5,49–51). Low affinity MBCs enter circulation early in an immune response (51), and higher-affinity MBCs continue to emerge as the GC reaction progresses (52). While GC-derived IgG MBCs on average are more somatically hypermutated (53), affinity-matured IgM MBCs also arise from GCs (54), and additional IgM MBCs are formed independent of a GC (55).

Murine studies reveal that GC-derived IgM MBCs contribute to the robust, rapid recall response to re-exposure that defines adaptive immunity (54,56). IgM MBCs in humans are beginning to be better appreciated for their roles in maintaining tolerance to gut commensals (57) and protection against pathogens (58–60). Our understanding of the substantial heterogeneity of MBCs (48) has been greatly expanded by work that seeks to distinguish various MBC subtypes based on ontology (55,56), surface-marker expression (61), transcriptional profile (62), and/or fate upon re-activation (63,64). While more specific distinctions will be made in some portions of the text, this thesis will generally employ a holistic, functional definition of MBCs: antigen-experienced, BCR-expressing cells that persist in a quiescent state following an initial immune response and maintain long-term antigen-responsiveness (51).

1.7 Methods for isolating antigen-specific MBCs

The use of MBCs for mAb discovery is challenged by technical barriers, the first of which is the low frequency of MBCs in peripheral blood. Only a small fraction of the total circulating peripheral blood B lymphocytes are MBCs, and those specific for any particular antigen are rarer

still (8,65). A success that nevertheless highlights the inefficiencies of a specificity-agnostic approach for mAb discovery, the anti-Ebolavirus mAb approved by the FDA in 2020 (ansuvimab (20)) was discovered using a blunt-force method of immortalizing 3 x 10^5 IgG^+ MBCs from a long-recovered subject who had markedly high neutralizing antibody titers (66). (Of note, antibodies in convalescent patients are supplied by long-lived plasma cells, and serum titers are not tightly correlated with the number of circulating (65,67,68) or lymphoid tissue (65) MBCs of similar specificity.) Forty Ebola-specific clones, including two with neutralizing activity, were ultimately identified (66). Experimental anti-Zika virus mAbs have also been generated without discriminating B cell subset, albeit in more recently-recovered subjects (69). Among cells successfully expanded in culture, supernatant from 0.5% of clones bound to the target antigen. The ability to isolate antigen-specific MBCs has enabled discovery of promising therapeutic candidate mAbs that target *P. falciparum* (70–72) and HIV-1 (73,74). We likewise began our searches for protective mAbs in blood samples from previously-exposed human subjects, using methods that begin with antigen-specific MBCs, and broadening our search to include multiple isotypes.

Fluorescently-labeled monomeric bait proteins can be used to identify B cells of a desired specificity (75). Unfortunately, bait-bound cells can be difficult to distinguish from non-specific cells, a problem exacerbated by the rarity of antigen-specific cells at later timepoints following infection (76). Further, as MBCs have reduced BCR expression relative to naïve or recently activated B cells (77), enrichment strategies that use single protein baits advantage non-MBCs, and exclude low- to moderate-affinity BCRs that contribute to the repertoire. Therefore, we prefer to enrich using tetramer reagents made with biotinylated target at 4:1 ratio with streptavidin-linked fluorophore (56,78). Importantly, pre-incubation with a labeled decoy tetramer allows exclusion of promiscuous or fluorophore-binding B cells (56,78).

In the next chapters, we used target-fluorophore tetramers to enrich, label and isolate antigen-specific MBCs. In Chapter 2, I isolated pathogen-specific B cells using a novel tetramer reagent generated by K.K. Takehara (Pepper lab; University of Washington). In Chapter 3, we use a tetramer approach coupled with phenotypic data from surface staining to distinguish IgM MBCs *vs*. IgG MBCs targeting the same antigen.

1.8 CAN BCR SEQUENCES BE OBTAINED EFFICIENTLY FROM SINGLE MBCS USING OPTIMIZED METHODS?

Single cell BCR sequencing is slow and technically challenging relative to other strategies (27). Our group first cloned single cell BCR sequences to generate purified mAbs more than a decade ago, for the purposes of better understanding B cell repertoire development and homeostasis (79). Since then, C.D. Thouvenel (Rawlings lab; University of Washington) has continued to refine, expand, and increase the efficiency of BCR cloning methods in mice (54) and humans (58,80). In Chapter 2, I employed a newly developed third-generation sequencing pipeline. A paper describing the method in greater detail is also being prepared for publication.

In Chapter 2, sequences derived from *P. aeruginosa*-specific MBCs of multiple isotypes (IgM, IgA, and IgG) were expressed as mAbs. In Chapter 3, 26 virus-specific IgM MBCs were isolated and sequenced in donors after recovery from mild COVID-19 illness. A highly-potent neutralizing IgM mAb is generated based upon BCR sequencing of a SARS-CoV-2-specific IgM MBCs. Eight neutralizing mAbs previously derived from IgG MBCs (81) in the same donors were also further explored.

1.9 Can IgM MBC BCRs be expressed as IgM mAbs?

Traditional hybridoma screening methods are generally isotype-agnostic, and IgM-producing cells may arise among the best clones (82). However, as IgM is considered technically challenging to produce and purify (83), antigen-specific BCRs are cloned directly into IgG expression plasmids, regardless of source isotype (84,85). Methods developed by Y. Chen in our lab that optimized the heavy- to light-chain ratio and refined the purification process on commercial affinity columns (58) yielded the consistent, high-quality preparations of pentameric IgM required to perform our studies.

1.10 How can mAbs retain efficacy against evolving pathogens?

The work described here coincided with unprecedented interest in the development of new mAbs for the treatment of infectious disease (47) due to the outbreak of the COVID-19 global pandemic. Unfortunately, the rapidity with which new anti-SARS-CoV-2 mAbs reached clinical use was largely outpaced by the rapidity with which resistant viral variants achieved widespread circulation (86–88). *De novo* viral escape was also reported within individual patients after mAb treatment (89). mAbs binding so-called highly conserved targets were challenged by poorly accessible epitopes and high minimal inhibitory concentrations and did not reach clinical application (88).

In the hopes of preventing immune escape, some anti-SARS-CoV-2 mAbs were packaged as cocktails (47,88). Regeneron's two mAb cocktail (REGN-CoV2) was given FDA emergency use authorization in November 2021. By the time of its approval, however, several circulating variants already carried mutations that evaded casirivimab, rendering it essentially a monotherapy (87,90). Three months later, the dual-resistant omicron variant rendered it impotent (91,92).

Anti-viral mAb cocktails have also been attempted against other pathogens, including HIV-1 (93) and Ebola (25). While SARS-CoV-2 was a special challenge due to the high prevalence of infection globally, HIV-1 is arguably the worst-case scenario for immune escape, due to the extraordinary rate of mutation and significant reservoir within individual patients. The relationship of HIV-1 to established broadly neutralizing antibodies (bNAbs) within the population of HIV-infected people has seen slower drift toward resistance to known neutralizing antibodies (94,95) than for the more common and more-recently-emergent SARS-CoV-2. Combinations of bNAb mAbs retain *in vitro* neutralization when used as a cocktail (94,95). Encouragingly, HIV-1 viremia initially plummeted in a recent high-profile trial of a 3 bNAb cocktail (93). However, 20 days after infusion, viremia began to rise. When sequenced, rebounding virus was resistant to 2 of the 3 mAbs. In short, simultaneous delivery of multiple IgG mAbs alone may not be a sufficient strategy for preventing immune escape.

In Chapter 3, we show that pentameric IgM mAbs retain activity against SARS-CoV-2 variants that escape recognition by IgG mAbs with identical variable regions. By increasing valency from 2 (IgG) to 10 (IgM), enhanced avidity compensates for reduced affinity. This and additional advantages of IgM mAbs are discussed further in Chapter 3.

1.11 Outline of goals and hypotheses

Overall hypothesis: IgM memory provides protection from diverse pathogens.

1) Hypothesis – Chapter 2: MBCs, including IgM MBCs, that recognize an important *P. aeruginosa* virulence factor (PcrV) are present in patients with cystic fibrosis.
2) Hypothesis – Chapter 3: IgM MBCs in COVID-19 convalescent subjects encode neutralizing antibodies against SARS-CoV-2.

Overall hypothesis: MBC BCR sequencing will enable efficient discovery and optimization of human mAbs with clinically-relevant protective activity against important human pathogens.

1) Hypothesis – Chapter 2: Protective anti-*P. aeruginosa* mAbs can be generated using sequences found in cystic fibrosis B cells.
2) Hypothesis – Chapter 3: Multimerization as IgM will enhance the neutralizing activity of mAbs against diverse SARS-CoV-2 variants.

Chapter 2. Monoclonal antibodies derived from B cells in subjects with cystic fibrosis protect against infection by *Pseudomonas aeruginosa*

An adapted and expanded version of this chapter is being prepared for publication as:

Hale M, Takehara KK, Thouvenel CD, Moustafa DA, Repele A, Fontana M, Netland J, McNamara S, Gibson RL, Goldberg JB, Rawlings DJ, Pepper M. Monoclonal antibodies derived from B cells in subjects with cystic fibrosis protect against infection by Pseudomonas aeruginosa.

2.1 INTRODUCTION

Pseudomonas aeruginosa (PA) is a ubiquitous, gram-negative bacteria responsible for significant morbidity and mortality in vulnerable individuals. Treatment is challenging because of intrinsic and acquired antibiotic resistance to most antibiotic drug classes (96). PA is one of the most common pathogens in severe healthcare associated infections (97). Due to the significant mortality caused by multi-drug resistant strains and the lack of alternative therapies, new anti-pseudomonal medicines are urgently needed.

Monoclonal antibodies (mAbs) that bind to key PA virulence factors have shown promise in animal models. PcrV is a 28kDa surface protein that forms the distal tip of the type III secretion system (T3S) required for the toxin injection into host cells (98). A humanized anti-PcrV antibody fragment (Fab) (99,100) and a bi-specific containing an anti-PcrV binding moiety raised in transgenic mice (101,102) have demonstrated safety in ventilated patients at high risk for PA pneumonia, but each failed to achieve the targeted efficacy outcomes in Phase 2 trials. Based on the evidence for protection by species-concordant mAbs in animal models of PA pneumonia and safety and suggestions for partial efficacy of early candidate mAbs in clinical trials, pursuit of improved anti-PcrV therapies for use in humans remains attractive.

In prior studies of Covid-19 and malaria, our groups have generated potent anti-pathogen mAbs by sequencing the variable regions of the proto-antibody B cell receptor (BCR) in antigen-specific memory B cells (MBCs) that arise following natural infection in humans (58,81,103). Therefore, we hypothesized that protective anti-PcrV monoclonal antibodies might be derived from B cells in individuals previously infected with PA.

Persons living with cystic fibrosis (CF) experience frequent airway PA infections. Intermittent infections early in childhood eventually progress to a state of persistent, chronic

airway colonization. CF is a multi-organ disease caused by mutations in the gene encoding CFTR, an ion channel. Several mechanisms related to the biology of the CF airway have been proposed to explain susceptibility to PA. Importantly, mutations in CFTR do not produce intrinsic deficits in adaptive immunity. Class-switched anti-PcrV antibodies are present in CF serum and sputum, at higher concentrations than the general population (104,105). However, the PcrV-specific B cells that give rise to antibody-secreting cells have not been previously studied. Here, we show that individuals with CF have more PcrV-specific circulating B cells. Building on this finding, we utilized single-cell sequencing to reveal PcrV-specific paired-chain BCR sequences in CF subjects. From BCR sequences derived from CF plasmablasts and MBCs, we generated novel anti-PcrV mAbs, including several that confer robust protection against a virulent strain of PA in an *in vivo* pneumonia challenge model.

2.2 RESULTS

2.2.1 *PcrV-specific B cells are enriched in CF individuals*

To prepare to isolate PcrV-specific cells, we first generated antigen-specific tetramer reagent consisting of four recombinant PcrV proteins linked to a fluorophore. In parallel, we also generated a decoy tetramer consisting of irrelevant proteins linked to a tandem fluorophore (**Figure 2.1 A**). To test the tetramer reagent, we immunized immune competent mice with recombinant PcrV. Immunization induced class-switched B cells that bound to the tetramer, findings consistent with successful detection of cells derived from a PcrV-specific germinal center response, and implying that this reagent should function similarly for detection of antigen-specific human B cells (**Figure 2.2**).

We next obtained peripheral blood samples from a cohort of 14 young adults with CF who had received a swab test for PA as part of routine outpatient care. As B cells specific for any single antigen are rare, tetramer-bound cells were enriched via an anti-fluorophore magnetic column prior to analysis. After enrichment, PcrV-specific cells made up ≥ 5% of B cells in 7 of 14 (50%) of CF donors, while 0 of 14 (0%) samples obtained from non-CF donors (isolated from a local blood bank) exhibited binding (**Figure 2.1 B**). Similar differences between CF *vs.* non-CF donors were obtained when the number of PcrV-specific B cells in each sample was normalized to lymphocyte count (**Figure 2.1 C**).

2.2.2 *Generation of mAbs from IgM$^+$ B cells derived from a CF donor with chronic PA pulmonary infection*

To initially test the ability to isolate PcrV-specific cells, we performed studies using a blood sample from an additional CF donor (Donor 1), who was known to be chronically PA-infected. Following single cell sorting of PcrV-specific cells, we performed paired chain sequencing of the heavy and light chain variable regions. Our FACS sorting method allows single-cell surface phenotyping data to be linked to the BCR sequence for individual cells. Interestingly, PcrV-specific B cells were rare, and only a very small number of PcrV-specific B cells expressed the canonical MBC surface markers ($CD21^+CD27^+$). Consistent with these observations, BCR sequencing of PcrV-specific B cells revealed predominantly germline sequences with little or no evidence for somatic hypermutation (**Figure 2.3 A**).

To directly confirm the specificity of newly acquired variable region sequences, we generated mAbs that employed the BCR variable regions from 10 of the tetramer-bound B cells isolated in this donor. As the surface-expressed isotype of all these PcrV-specific B cells was IgM, we first expressed the BCR sequences as pentameric IgM antibodies. When tested for binding to

recombinant PcrV in a plate-bound ELISA assay, supernatants collected from cells co-transfected with heavy, light, and J chain plasmids (to make pentameric IgM) exhibited strong binding to PcrV for 3 of 10 CF-derived BCRs (**Figure 2.3 B**). The light chain for BCR 421 contains several mutations in CDR1. We were especially intrigued by the apparently strong binding by germline antibody sequences 408 and 411. The source cells for 411 and 421, but not 408, expressed a surface marker suggestive of a plasmablast/plasma cell phenotype ($CD38^{+}$).

As clinical application was likely to require large-scale production in a similar system, we chose to move forward with the best binders that also were most efficiently expressed in the 293T cell line: 408 and 411.

We have previously found that for mAbs that target divergent pathogens, including SARS-CoV-2 and *Plasmodium falciparum*, multimerized antibodies (eg. pentameric IgM) have enhanced binding and protection properties *in vitro* (58,103). However, nearly all current monoclonal antibody therapeutics employ the IgG1 isotype (106). Therefore, we next sought to compare the activity of these mAbs in both the IgM and IgG1 formats, and generated expression plasmids containing the heavy chain variable regions upstream of the gamma1 constant region to enable expression as IgG1 mAbs. After co-transfection with the paired light chain (+ J chain for IgM) and antibody purification, we were able to compare binding to recombinant PcrV for BCR sequences 408 and 411 when expressed as IgG *vs*. IgM mAbs (**Figure 2.3 C**). CF BCRs 408 and 411 exhibited binding to PcrV as both IgM and IgG mAbs; with higher binding as IgM, presumably reflecting the avidity of IgM multimers.

One challenge in studying new candidate human PcrV mAbs is the lack of readily available comparators. V2L2MD is a heavily engineered anti-PcrV mAb that was generated by phage display binding optimization from a pre-cursor candidate identified by hybridoma screening from

PcrV-immunized, human-variable region transgenic mice (101). The clinical candidate bi-specific, gremubamab, consists of the paired heavy-and light chain variable regions of V2L2MD fused to an anti-polysaccharide (Psl) single chain variable fragment (scFv) and the human IgG1 constant region (39,102). To prepare for *in vivo* protection assays, we introduced gremubamab's anti-PcrV variable regions (V2L2MD) into expression plasmids using the same strategies we have employed for expressing CF BCRs. This approach enabled us to produce and purify positive control human V2L2MD IgG and IgM mAbs in parallel with our candidate CF BCR-derived mAbs. To confirm specificity, we measured binding to recombinant PcrV for purified IgG and IgM mAbs produced in parallel from CF BCR 411 and the newly cloned V2L2MD, together with commercially sourced gremubamab (**Figure 2.3 D**). As IgM mAbs, CF BCR 411 and V2L2MD exhibited similar binding to PcrV, on par with the commercial gremubamab.

2.2.3 *Anti-PcrV mAbs derived from CF B cells protect mice from PA pneumonia*

Next, we used a challenge model of pneumonia (107) to test the anti-PA activity of candidate mAbs. Mice treated with a single, 60 μg intranasal dose of anti-PcrV IgG exhibited an ~ 2 log reduction in burden of bacteria in the lungs at 48 h in comparison with an off-target control mAb or vehicle (PBS) only (**Figure 2.4 A**). A similarly dramatic reduction in lung bacteria load was also achieved when the experiment was repeated with a 3-fold lower dose of anti-PcrV IgG (**Figure 2.4 B**). The CF-derived mAbs performed equivalently to the positive control V2L2MD mAb at both doses. While assessment of lung bacterial burden requires sacrifice of the treated mice, doses achieving similar reductions in lung bacterial burdens have resulted in 100% survival in cohorts of mice in prior studies of V2L2MD (101).

2.2.4 *Anti-PcrV mAbs derived from MBCs of individuals with CF*

The above findings demonstrate that isolation of PcrV-specific B cells chronically infected CF donor enabled the rapid discovery of 2 protective mAbs. Notably, these mAb were derived from B cells lacking an MBC phenotype. In our earlier studies of other pathogens, antigen-specific MBCs had been excellent sources for high-affinity, protective BCR sequences (58,81). Therefore, we were eager to investigate whether additional, and perhaps, higher affinity, anti-PcrV mAb could be isolated from antigen-experienced, somatically hypermutated, PcrV-specific MBCs. Unfortunately, PcrV-specific MBCs were extremely rare in the subject who we had initially selected for BCR sequencing (**Figure 2.3 A**). Therefore, we obtained peripheral blood samples from 2 additional donors with CF: Donor 2, had previously tested positive for PA but was negative on most recent testing, while Donor 3, like Donor 1, was chronically infected. Using improved methods that enhanced the efficiency and depth of sequencing (manuscript in preparation as Thouvenel et al.), we performed single cell BCR sequencing of PcrV-specific B cells from each donor. Strikingly, Donor 2, had abundant PcrV-specific MBCs after tetramer enrichment. Of the ~ 40 sequences from PcrV-specific cells identified by surface phenotype as likely MBCs ($CD21^{+}CD27^{+}$), many were somatically hypermutated (**Figure 2.5 A**). In contrast, Donor 3 had fewer MBCs and fewer somatically hypermutated cells (**Figure 2.6 A**).

There was significant breadth in V family usage within and between donors (**Figure 2.6 B**). The small number of cells analyzed, compared to B cell repertoire studies that employ bulk sorted populations, limits the interpretation of our data. However, a strength of singly sorted B cell sequencing is the ability to obtained paired chain information. The heavy chain IGHV3-23 is used, with mutations, in the V2L2MD antibody, and is a very common VH gene segment in most human B cell repertoire studies (108). Accordingly, it was not surprising that IGHV3-23 was also

well represented in this dataset. Notably, none of the PcrV-specific B cells sequenced for our study paired VH3-23 heavy chains with IGKV1-6, the V2L2MD light chain variable gene (**Figure 2.6 C**) and IGKV1-6 was infrequent in our dataset. Heavy- and light-chain pairings for $CD21^{+}CD27^{+}$ cells are shown in **Figure 2.5 B**. These data represent the first attempt to sequence human PcrV-specific BCRs.

To pursue our goal of identifying potential protective mAbs among MBCs, 12 of these BCRs were randomly selected for cloning into expression plasmids. Supernatants from transfected cells were screened for binding to PcrV (**Figure 2.7**). BCRs 435 and 442 were the most striking binders in the transfection screen. Because our initial screen did not adequately control for antibody concentration in the supernatant, antibodies that are less efficiently expressed by 293T cells might appear to be poor binders. Based on performance in the screen or for reasons of special interest (*eg.* BCR clone 439 was derived from an IgA MBC, the predominant isotype in respiratory secretions), 5 MBC-derived BCRs were chosen for production as purified IgG mAbs. When this panel of purified mAbs was evaluated at matched concentrations (**Figure 2.5 C**), 2 of 5 of MBC-derived mAbs matched or exceeded PcrV binding exhibited by the protective, donor 1 (plasmablast derived) mAb, 411. Further, 4 of 5 (including the IgA-derived mAb, 439) matched or exceeded the other protective donor-1 derived protective mAb, 408 IgG.

2.3 FIGURES

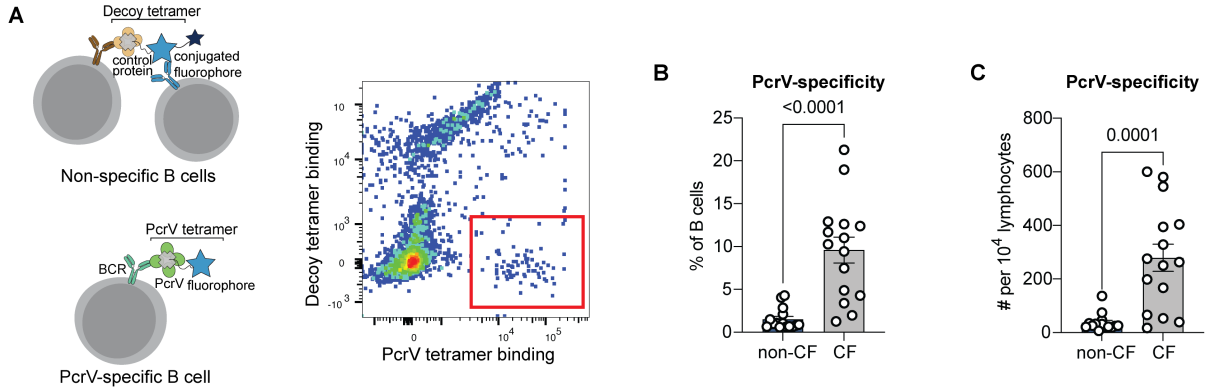

Figure 2.1. PcrV-specific B cells in subjects with cystic fibrosis (CF). A) Schematic of primary human B cells binding to PcrV tetramer reagent and decoy (left). Representative flow plot for B cells after enrichment. Cells binding only to the PcrV tetramer are indicated with the red box. B-C) Percentage (B) and frequency (C) of PcrV-specific B cells in 14 human subjects with cystic fibrosis (CF) vs. control, blood bank donors (non-CF).

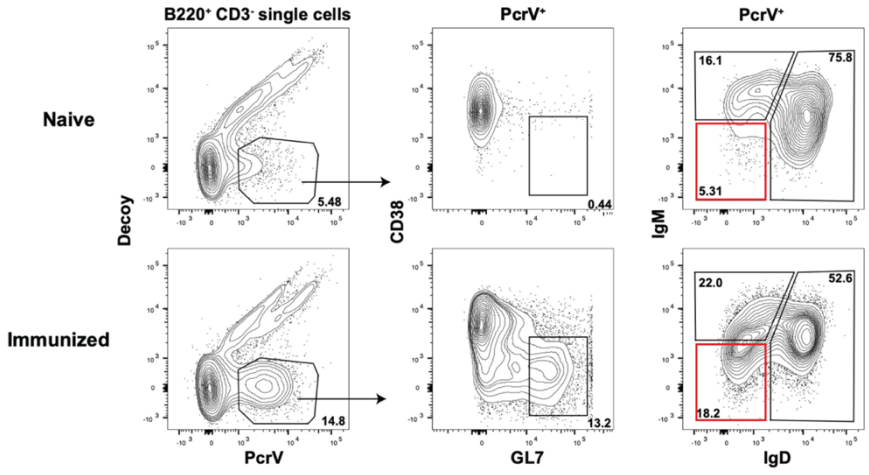

Figure 2.2. Tetramer-specific class-switched B cells in mice immunized with PcrV. Flow cytometry plots from lymphoid tissue in representative PcrV-immunized or control (naïve) mice sacrificed on day 7 post-immunization by intraperitoneal injection. Cells were analyzed after the

magnetic enrichment of tetramer-bound cells. Class-switched B cells are highlighted within the red boxes.

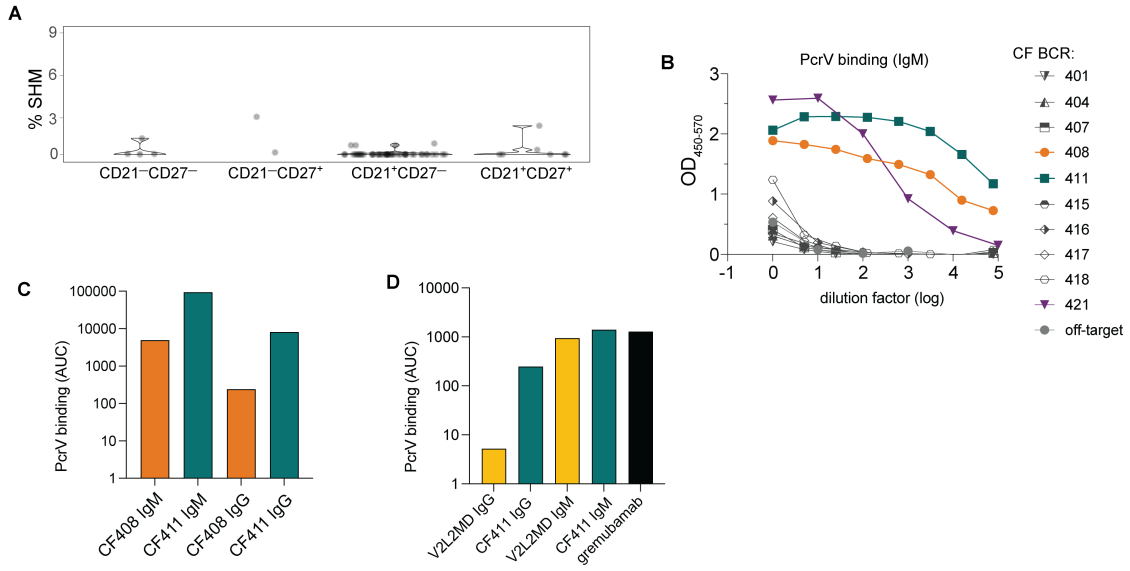

Figure 2.3. **Generation of anti-PcrV mAbs derived from B cells isolated from a chronically PA infected CF donor.** A) Percentage of somatic hypermutation (SHM) detected in B cell receptor (BCR) sequences from cells of the indicated phenotype for CF donor 1. B) ELISAs showing PcrV binding using supernatants derived from 293T cells transfected with IgM expression plasmids containing the indicated BCR sequences. C) Area under the curve (AUC) for representative ELISAs of purified antibodies 408 and 411 expressed alternatively as IgM vs. IgG. D) AUC for representative ELISA of purified mAbs V2L2 and 411 expressed, alternatively as, IgG vs. IgM; and for the commercially sourced, clinical, bi-specific mAb, gremubamab. mAbs derived from CF subject B cells are labeled with the CF prefix for clarity.

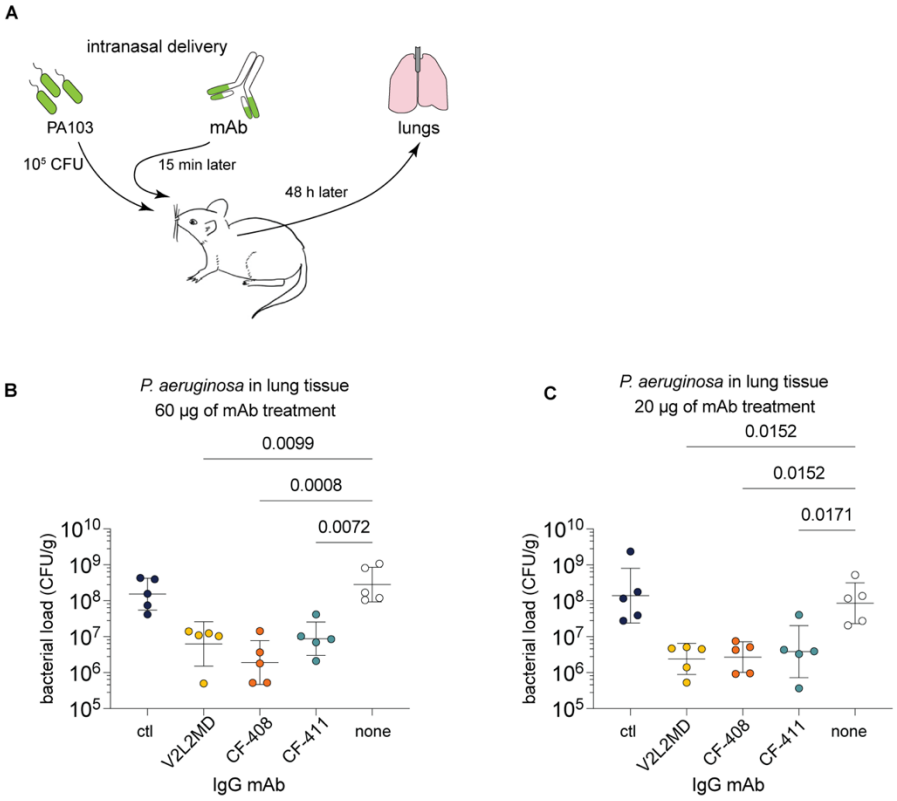

Figure 2.4. **CF-subject derived, germline, anti-PcrV-specific mAbs exhibit robust anti-PA activity in an *in vivo* mouse pneumonia model.** A) Schematic illustrating the experimental PA infection and mAb delivery protocol. B-C) Bacterial load in mouse lungs at 48 h post-infection for mice that received a 60 µg (B) or 20 µg (C) intranasal dose of off-target, control IgG1 mAb (ctl), indicated anti-PcrV mAbs, or diluent alone (none).

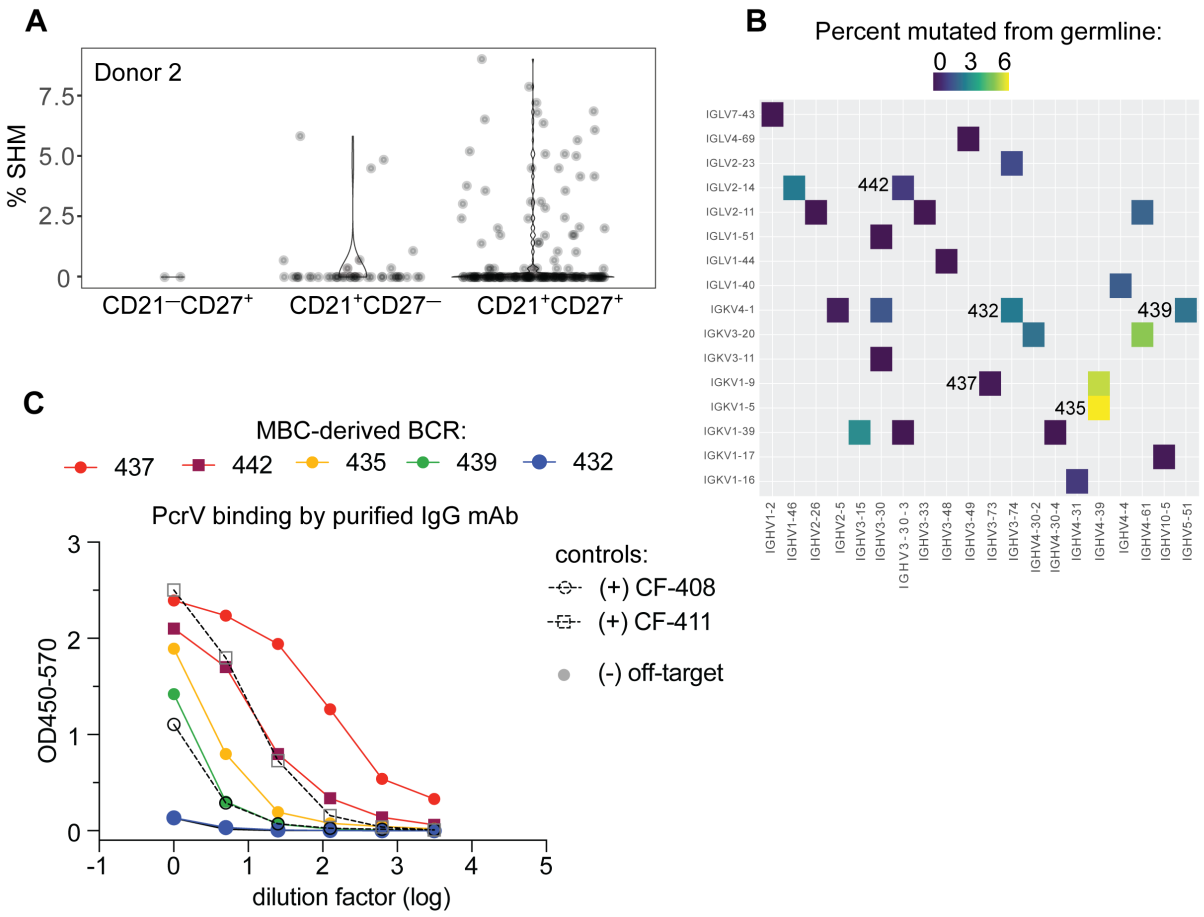

Figure 2.5. High affinity anti-PcrV mAbs derived from memory B cells isolated from CF Donor 2. A) Somatic hypermutation (%SHM) rates in BCR sequences from individual B cells with the indicated surface phenotype isolated from CF donor 2. Each circle represents a singly sorted cell. B) Heatmap showing paired heavy (x-axis) and light (y-axis) V gene families for 31 MBCs in donor 3. The color gradient depicts SHM for the heavy chains in each pairing. Clone numbers for BCRs to be expressed as mAbs are included to the left of their corresponding box. C) PcrV binding by ELISA for purified mAbs generated from five MBC BCRs (colored lines). The two CF subject 1-derived mAbs with *in vivo* protective activity (CF 408 and CF 411) are used as benchmarks for relative binding activity (dashed lines). The off-target control (anti-SARS-CoV-2 RBD) line appears hidden because it overlaps with the blue line (CF 432).

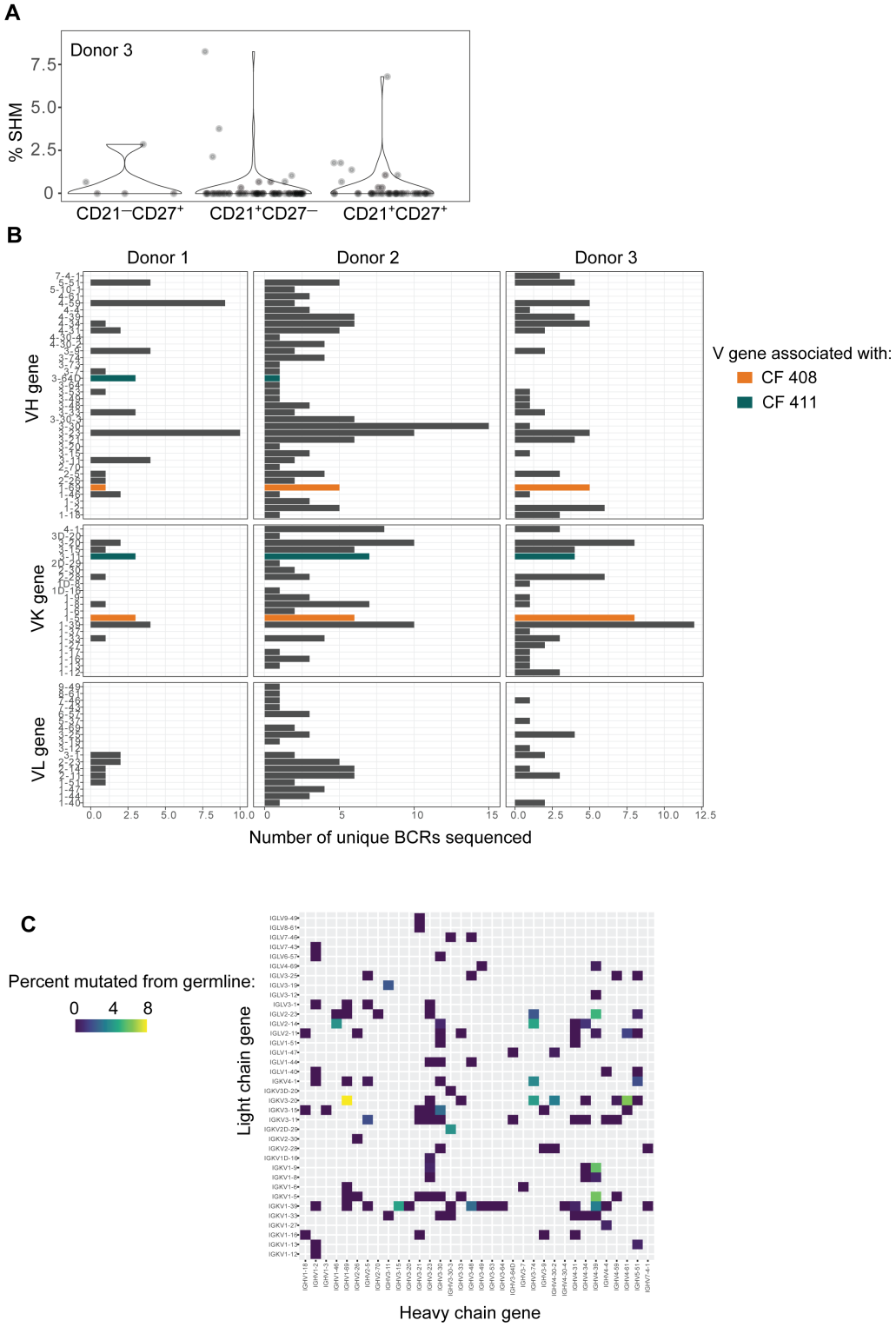

Figure 2.6. B cell receptor (BCR) sequencing of PcrV-tetramer-specific B cells derived from 3 CF donors. A) Percentage of somatic hypermutation (SHM) detected in BCR sequences

from cells of the indicated phenotype in chronically PA infected, CF donor 3. Each circle represents a singly sorted cell. B) Histograms show the number of unique BCR sequences obtained for each V gene family (y-axis) for heavy and light (kappa or lambda) chains. Data from each CF donor is shown in a separate panel of graphs (with Donor number indicated at top). The bars for the V gene families used by *in vivo*-tested mAbs are colored as: blue-green (CF 411) and orange (CF 408). C) Heatmap showing pairings of heavy- (x-axis) and light (y-axis) chain V gene families where with full-length, high quality V region sequence was attained. For each heavy/light chain pair, the percentage of heavy chain sequence which differs from the germline sequence is depicted by color gradient.

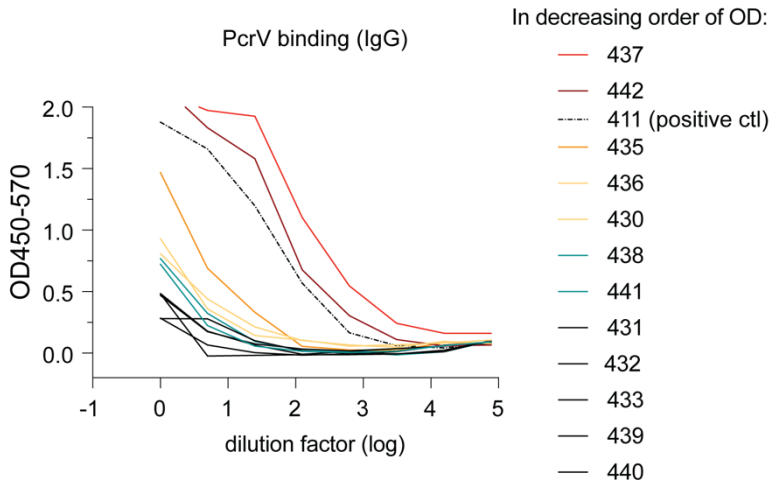

Figure 2.7. **Transfectant supernatant screen of 12 MBC-derived mAbs.** ELISA assessing PcrV binding for supernatants from 293T cells transfected with IgG expression plasmids. Numbers (430-442) indicate the BCR sequences identified from individual, PcrV-specific, MBCs from CF donor 2. Supernatant for mAb 411 IgG (dotted line; isolated from CF Donor 1) is included as a benchmark (positive ctl).

2.4 DISCUSSION

In the face of rising antibiotic resistance by pathogenic bacteria, the development of new antimicrobial treatment modalities becomes increasingly desirable. Because mechanisms of intrinsic resistance already limit therapeutic options, multidrug-resistant PA can be especially difficult to treat (109). Unfortunately, relative to the projected need, few novel antimicrobials are under active pharmaceutical development (2). Antimicrobial mAbs may fill a widening gap as alternatives, or adjuncts, to traditional antibiotics. Efforts to develop mAbs for PA antibodies targeting PcrV, a critical component of the toxin injection apparatus, are bolstered by strong evidence for antibody-mediated protection in animal models (110–113). Unfortunately, two engineered antibody-like drug candidates (a Fab fragment and a bi-specific) derived from mice failed to achieve positive end points in Phase II trials (102,109,114). Thus, new work is required to identify human mAbs that would improve on immunogenicity risk and pharmacokinetics, while maintaining robust protective activity.

Traditional methods of mAb development require extensive labor in the early stages, from immunization of mice with a recombinant protein to screening hundreds of hybridomas. Further, to address the immunogenicity of the murine constant region, mouse-derived antibodies must be iteratively re-humanized *in vitro* and/or modified into antibody fragments (Fab) which lack effector functions and are subject to rapid renal clearance. Although fully *in vitro* strategies like phage display can enable the use of human variable domains (115), the high-throughput screening processes are vulnerable to bottleneck effects and drift, do not select against autoreactivity or immunogenicity, and do not screen paired VH/VL sequences within the context of full-length paired chains. An alternative approach that has also sought to maximize throughput in screening

for high affinity anti-PcrV binders from a library of llama-derived nanobodies (116) shares similar advantages and drawbacks.

Here, we generated multiple anti-PcrV mAbs directly from the BCR variable regions of antigen-specific B cells derived from CF donors. For practical reasons, we tested only a subset of paired antibody sequences that were isolated from single cells. Overall, while lower throughput than library screens, antibody discovery was extremely efficient, requiring expression of very few (< 12) BCRs to yield high-affinity anti-pseudomonal mAbs from each of 2 donors. Interestingly, sequences encoding protective IgG mAbs were obtained from a phenotypically diverse set of B cells, including class-switched and IgM MBCs and IgM-expressing cells that lacked canonical MBC markers and employed fully germline BCRs. Strikingly, the two tested mAbs directly cloned from human B cells achieved control of PA infection that matched V2L2MD IgG, the PcrV-specific binding component of gremubamab. Notably, promising results in animal models may not predict clinical success for novel anti-PA therapeutics. However, mAbs derived from human B cells have theoretical advantages *vs.* previously trialed KB001 and gremubamab that would not be reflected in murine models, including reduced immunogenicity and fully human effector functions.

While the goal of this study was to generate novel protective mAbs for therapeutic use, our findings have an additional benefit of insight into the biology of the adaptive humoral response to PA in CF, which has thus far been limited to comparing titrations of secreted antibodies (104). As we hypothesized given the uniquely high frequency of PA infections in the CF population, circulating PcrV-specific B cells in CF individuals were expanded compared to non-CF individuals, a finding that raises interesting new questions about barriers to clearance of infection. While the ability to generate protective mAbs *ex vivo* from single cell CF BCRs demonstrates that B cells with the technical capacity to produce functional anti-PA antibodies, while rare, are present

in the peripheral blood, multiple *in vivo* challenges may limit PA clearance in individuals with CF. Significant future work will be required to fully characterize the nature and dynamics of PA-specific B cells in CF individuals. Better understanding of the endogenous anti-PA response might also reveal insight that could enhance future therapeutic antibody products.

We have previously shown that protective mAbs may be built from antigen-specific MBCs that target the parasite *Plasmodium falciparum* and the virus SARS-CoV-2 (58,81,103). Besides eliminating the humanization requirement and concern for residual immunogenicity, human MBC-derived mAbs are the product of evolved B cell development and maturation processes that encompass tremendous diversity and include selection against auto-reactivity and, for cells that have exited GCs, pre-optimized binding to antigen via affinity maturation. When combined with the results of our present study, human antigen-specific B cells may be broadly considered as an underutilized high-yield resource in the critical endeavor to discover new treatments for infectious disease.

2.5 Materials and Methods

PBMC and serum collection

Under protocols approved by the Seattle Children's Institutional Review Board (SCH#10325), CF donors were recruited from patients receiving care that day at Seattle Children's Cystic Fibrosis Clinic in March-June 2019 (for initial B cell phenotyping and serum ELISAs) and April-July 2021 (serum ELISAs and BCR sequencing experiments). Individuals who declined to participate or were assessed by the clinical team to be unable to safely donate at least 30 mL of blood were excluded. Blood was transported at room temperature to the University of Washington Department of Immunology and processed within 4 hours of collection. Serum was collected by

centrifugation at 1500 g for 10 min, and then frozen at -80 C. Peripheral mononuclear blood cells (PBMCs) were collected using SepMate-50 PBMC Isolation Tubes (STEMCELL Technologies) and frozen slowly at -80 C before transfer to liquid nitrogen for long-term storage. Non-CF donor samples were provided by BloodWorks Northwest from regular blood donors or from non-mobilized healthy donors through the Fred Hutch Hematopoietic Cell Procurement and Processing core.

Tetramer production

Recombinant PcrV was expressed using *E. coli* transformed with low copy plasmid containing the PcrV CDS (GenBank: AF010149.1) and a 10 X N terminal His tag, and purified from filtered bacterial supernatant on a His affinity column. To enable tetramerization, PcrV was biotinylated using EZ-Link Sulfo-NHS-LC Biotinylation Kit (ThermoFisher). The production of antigen-specific B cell tetramer reagents has been previously described in some detail (78). Briefly, biotinylated PcrV was co-incubated with streptavidin-fluorophore (SA-PE or SA-APC; Agilent). Decoy tetramers are produced by tetramerization of an irrelevant protein with a matched conjugated fluorophore (eg. PE-Cy7 for use in experiments requiring the PE-conjugated PcrV tetramer).

Identification of PcrV-specific cells

Our methods for isolating antigen-specific B cells using tetramer reagents are described in detail elsewhere (78). Flow cytometry was performed on a BD LSR II (Becton Dickinson). For BCR sequencing experiments, single cells were sorted into a 96 well-microplate using a BDFACS Aria II that was contained within a biosafety cabinet.

BCR sequencing

cDNA was amplified from singly sorted B cells using SMART-Seq v4 (Takara Bio) at half reaction volumes. Initial BCR sequencing for donor 1 followed protocols we have previously described in detail (58,81,103). Briefly, a single, multiplex PCR was performed for each B cell using a universal primer for the template switch region and pooled constant region primers for the μ, γ, α, κ, and λ constant regions. Amplicons were then purified and sequenced by Sanger sequencing. For donors 2 and 3, a custom protocol that enables high-quality, single cell BCR sequencing by MiSeq was employed (manuscript in preparation as Thouvenel et al). Alignment of all trimmed sequences was performed using both TRUST4 (117) and IGMT/HighV-QUEST (118). Rare conflicts (*eg.* differences in reported %SHM) were resolved by review of the raw sequence data and individual analysis in IgBlast (119).

BCR cloning

Our methods for cloning BCR variable region sequences into antibody expression plasmids were described previously (58,81,103). Briefly, each light chain was cloned into vectors of its isotype, κ or λ, following the manufacturer's protocol for in-fusion cloning (Takara Bio). All heavy chains were similarly cloned into IgG1 and IgM plasmids in parallel. Concordance with the parental cDNA was confirmed by Sanger sequencing of the cloned plasmids.

For the V2L2MD IgG and IgM mAbs, heavy and light chain sequences were synthesized as a gBlock (IDT) by introducing mutations to match the amino acid sequence for the anti-PcrV VH/VL in gremubamab (INN 10909; 17) in the closest human VH and VL nucleotide sequences. The resultant V(D)J sequences were then synthesized as a gBlock (IDT) and then cloned into

expression plasmids using the same methods described for generation of our human B cell BCR sequences.

Whole-plasmid sequences were obtained from a subset of plasmids as a quality control measure (Primordium Labs).

Production of mAbs

IgG mAbs were produced in HEK-293T cells (ATCC) by co-transfection of heavy- and light-chains in polyethylenimine as previously described (58). Production of IgM mAbs was carried out as described in Hale et al., using the same human J chain plasmid. For initial screens, supernatant was harvested at 4 days post-transfection and concentrated and buffer-exchanged into PBS using 50,000 MWCO Millipore Amicon Ultra-15 Centrifugal Filter units (Thermo Fisher Scientific). Purification was carried out following manufacturer's instructions on HiTrap Protein G HP purification column for IgG mAbs (GE Healthcare), and a POROS CaptureSelect IgM-XL Affinity Matrix Column (Thermo Fisher Scientific) for IgM. Antibodies were concentrated and buffer-exchanged into phosphate buffered saline to at least 1 mg/mL, and then stored at -80C in 120-200 µL aliquots.

ELISAs

To prepare for antigen-specific antibody ELISAs, recombinant PcrV was prepared as described above and diluted to 2 µg/ml in PBS and incubated on high-binding 96 well plates (Corning) overnight at 4° C. Plates were then washed thoroughly with PBS and 0.05% Tween 20 (PBS-T). Next, non-specific interactions were blocked using 200 µl/well of PBS-T with 3% bovine serum albumin (3%) at room temperature for 1 – 3 hours. Samples of interest were serially diluted

in PBS-T immediately prior to use. Dilution series for each sample were incubated on washed plates for 2 hours at room temperature. After thorough washing with PBS-T, bound antibodies were detected by incubation for 1 hour at room temperature with HRP-conjugated goat anti-human IgG (diluted 1:3000 in PBS-T; SouthernBiotech), IgM (1:1500; SouthernBiotech), or IgA (1:1500; ThermoFisher), washed again, and developed using 1× 3,39,5,50-tetramethylbenzidine (Invitrogen) and 1 M H_2SO_4. OD was measured on a SpectroMax i3X (Molecular Devices, San Jose, CA) at 450 and 570 nm, and $OD_{450-750}$ was analyzed in Prism (v9.5; GraphPad). When un-purified transfectant supernatants were used, ELISAs for total IgM or IgG were also performed in parallel using human uncoated IgM or IgG ELISA kits (Invitrogen), following manufacturer's instructions.

Murine pneumonia challenge

All animal procedures were conducted according to the guidelines of the Emory University Institutional Animal Care and Use Committee (IACUC), under approved protocol number PROTO 201700441. The study was carried out in strict accordance with established guidelines and policies at Emory University School of Medicine, and recommendations in the Guide for Care and Use of Laboratory Animals, as well as local, state, and federal laws. Eight-to ten-week-old female BALB/c mice (Jackson Laboratories, Bar Harbor, ME) were anesthetized by intraperitoneal injection of 0.2 ml of a cocktail of ketamine (100 mg/ml) and xylazine (5 mg/ml) and intranasally instilled with approximately 10^5 CFU *P. aeruginosa* PA103 (in 10-20 µL of PBS). At 15 minutes post-infection, monoclonal antibodies or PBS were delivered via the same route in a 20 µl volume. Mice were euthanized at 24 hours post-infection, and whole lungs were collected aseptically, weighed, and

homogenized for 20 seconds in 1 ml of PBS, followed by serial dilution onto Difco™ Pseudomonas isolation agar, and plated for CFU enumeration.

Author Contributions

Conceptualization: M. Hale, K.K. Takehara, C.D. Thouvenel, D.A. Moustafa, M. Fontana, J.B. Goldberg, M. Pepper and D.J. Rawlings. Supervision/direction: S. McNamara, R.L. Gibson, J.B. Goldberg, M. Pepper and D.J. Rawlings. Funding acquisition: R.L. Gibson, J.B. Goldberg, M. Pepper and D.J. Rawlings. Investigation: M. Hale, K.K. Takehara, C.D. Thouvenel, D.A. Moustafa, A. Repele, M. Fontana and J. Netland. Data analysis: M. Hale, K.K. Takehara, C.D. Thouvenel, D.A. Moustafa, A. Repele, M. Fontana, J. Netland, M. Pepper and D.J. Rawlings. Writing - original draft: M. Hale. Writing - review and editing: M. Hale, M. Pepper and D.J. Rawlings.

Chapter 3. IgM antibodies derived from memory B cells are potent cross-variant neutralizers of SARS-CoV-2

This chapter is adapted from the following publication:

Hale M*, Netland J*, Chen Y, Thouvenel CD, Nabel KG, Rich LM, Vanderwall ER, Miranda MC, Eggenberger J, Hao L, Watson MJ, Mundorff CC, Rodda LB, King NP, Guttman M, Gale M, Abraham J, Debley JS, Pepper M, Rawlings DJ. IgM antibodies derived from memory B cells are potent cross-variant neutralizers of SARS-CoV-2. *Journal of Experimental Medicine.* 2022;219(9). doi:10.1084/jem.20220849

*These authors contributed equally.

3.1 INTRODUCTION

Antibody products such as convalescent plasma or engineered monoclonal antibodies (mAbs) provide passive immunity to SARS-CoV-2 and can protect vulnerable individuals from severe COVID-19 illness or death. IgM antibodies play a major and out-sized role in SARS-CoV-2 neutralizing capacity based on studies of pooled convalescent plasma, despite comprising only ~5% of the total antibody pool (7,59). IgM is a natural pentamer with 10 epitope binding sites, and *in vivo* effector functions well-suited to neutralizing an invading virus including activating complement and triggering activation of immune cells (121,122). However, anti-SARS-CoV-2 mAbs in clinical use predominantly employ the monomeric, bivalent IgG structure most extensively developed for treatment of cancer and autoimmunity (123).

Emerging variants of SARS-CoV-2 have incorporated new mutations within the immunodominant receptor binding domain (RBD) of the spike protein, leading to escape from neutralizing mAbs (87,124,125). While the identification of novel cross-variant neutralizing antibodies is one path forward, an alternative strategy would be to modify existing mAbs to be more tolerant of mutation. We previously found that naturally multimerized IgM or engineered hexameric IgG enhanced the protective function of two malaria-specific mAbs via the cumulative binding strength of multiple interactions with an antigen-coated surface due to avidity (58). Multimerization might therefore expand the functional range of an anti-SARS-CoV-2 mAb by compensating for reductions in affinity to a mutated RBD via enhanced avidity. Supporting this concept, artificial multimers can neutralize human immunodeficiency virus escape mutants, provided that the antigen binding domains are arranged such that cross-linking could occur across viral spike proteins (126). Notably, SARS-CoV-2 spike proteins are distributed with a density such that inter- and intra-virion crosslinking could theoretically be performed by IgM (9,127,128).

The role of IgM and IgM-expressing cells in the human immune system must be better understood to maximize the therapeutic potential of IgM antibodies. IgM antibodies and IgM^+ B cells are most appreciated in the early plasmablast response, providing a low-affinity humoral stop-gap until higher-affinity antibodies of other isotypes are generated. This later response includes class-switched antibody-secreting plasmablasts, memory B cells (MBCs), and plasma cells that emerge from germinal centers. Re-activation of antigen-specific MBCs results in antibody production that can rapidly control pathogen propagation (129). A predominant pool of SARS-CoV-2-specific IgG^+ MBCs and significantly smaller population of IgM^+ MBCs are formed following infection or vaccination (49,130,131). Despite intensive study of IgG^+ MBCs, relatively little is known about the role for IgM^+ MBCs in protection. Indirect evidence suggests that RBD-specific IgM^+ MBCs may be important contributors to protective immunity, as well as a potentially underappreciated source of B cell receptor (BCR) sequences with therapeutic utility as neutralizing mAbs (132–137). However, descriptions of the SARS-CoV-2 IgM^+ MBC repertoire are limited by the small number detectable in the blood at late timepoints and the technical challenge of producing high-quality pentameric IgM to study the BCR in its native isotype (83–85).

Our group has established robust protocols for BCR sequencing of rare, antigen-specific MBCs and production of purified IgM mAbs (54,58,81). We used these methodologies to compare the relative functional activity of an array of SARS-CoV-2-specific sequences expressed as multimeric IgM vs. monomeric IgG that targeted a broad range of RBD epitopes. We then assessed the panel of clonally identical IgM vs. IgG mAbs for cross-variant neutralization. We also sought to determine whether IgM^+ MBCs present in convalescent individuals encode antibodies that bind and neutralize SARS-CoV-2. Our combined findings suggest that IgM antibodies may play an

important and underappreciated role in protection against SARS-CoV-2 variants when the protective capacity of serum IgG and IgG^+ MBCs alone may prove inadequate.

3.2 Results and Discussion

3.2.1 *Pentameric IgM increases the potency of IgG^+ MBC-derived neutralizing antibodies*

For initial investigation into the effect of multimerization on SARS-CoV-2-specific antibodies, we employed eight neutralizing mAbs derived from RBD-specific IgG^+ MBCs isolated from convalescent individuals (81). Building on methods for studying the repertoire of antigen-specific MBCs, BCRs from individual RBD-specific B cells were sequenced and the specificity-determining heavy and light chain variable regions were cloned into expression plasmids as gamma1 (for the heavy chain) or kappa/lambda (light chain) constructs (58) and IgG mAbs derived from each BCR were purified from co-transfected cells. Each heavy chain variable sequence was also cloned into a plasmid upstream of the mu (IgM) constant region to prepare for multimerization studies.

To build our panel of candidates for multimerization, we chose six IgG mAbs that had been previously tested in SARS-CoV-2 plaque neutralization tests (81), with a range of half-maximal neutralization titers (NT-50; 5-540 ng/ml; **Fig. 3.1 A**). We selected two additional IgG mAbs (257 and 308) that had failed to block RBD from binding ACE2 in a plate-bound assay, with the goal of also testing the impact of multimerization across a range of epitopes, including antibodies targeting regions outside of the ACE2:RBD interface (81). Each mAb was affixed to a biosensor to assess RBD binding and dissociation by biolayer interferometry (BLI) to assess affinity. Affinities for RBD ranged from sub-picomolar (mAbs 297 and 305) to 6.2 nM (284) (**Fig. 3.1 A** and **B**). To confirm that these mAbs represented a range of RBD target sites, we measured

competition for RBD binding by BLI using a panel of Fabs and IgG mAbs with known epitopes (**Fig. 3.2** and **3.3 A**, summarized in **Fig. 3.1 C** and **D**). From the combined results, we predicted that 3 of 8 mAbs (284, 297 and 305) bound at the ACE2 interface with likely Class 1 or Class 2 RBD-specific binding moieties, using a classification scheme described by Barnes *et al*. (138). MAb 203 did not appear to bind at the ACE2 interface, but competed strongly with LY-CoV555, a Class 2 antibody, and partially with S309, the Class 3 antibody that is the basis for sotrovimab, suggesting binding near but not directly blocking the ACE2 binding site (139). MAb 207 was predicted to be a Class 3-like antibody. MAb 239 competed with the tight-binding but non-neutralizing Class 4 CR3022 antibody (140), and with C1C-A3, a recently described Class 4 antibody that binds outside of the ACE2 footprint at the conserved RBD core (141). Contributing to evidence of binding outside the ACE2 footprint, 257 and 308 competed only with C1C-C6, a Class 4-like neutralizing antibody (based on competition with CR3022) that also does not directly block ACE2:RBD interactions in protein-based assays (141). Together, the predicted target sites within RBD, affinities and neutralization potencies demonstrate that this panel's MBC-derived mAbs encompass a diversity of immunologically relevant neutralizing epitopes.

For expression as IgM mAbs, in addition to the light chain and mu heavy-chain plasmids, we included a plasmid encoding the human joining (J) chain that enables self-assembly into pentameric IgM, the predominant form in humans (58,121,142). We also confirmed appropriate size, hydrodynamic radius, and purity of pentameric IgM using size exclusion chromatography with multiple angle light-scattering (SEC-MALS, **Fig. 3.3 C**).

To compare the properties of IgM vs. IgG mAbs with identical specificities, we first measured neutralization potencies against a luciferase-encoding SARS-CoV-2 spike pseudotyped lentiviral vector (pseudovirus) (143). Pseudovirus was pre-incubated with IgM or IgG mAbs, and

then applied to ACE2-expressing 293T cells. Strikingly, multimerization as IgM lowered the concentration required to achieve a 50% reduction in infection relative to untreated controls (NT-50) for all 8 IgG^+ MBC-derived mAbs with impacts ranging from 3-23 fold (**Fig. 3.1 E)**. There is a large size difference between monomeric IgG (~150 kDa) and pentameric IgM (~970 kDa) (83). Thus, considered on a molar basis, neutralizing activity increased ~20-150 fold.

Relative effects for IgG/IgM pairs were not attributable solely to their RBD epitope. In particular, if, as has been speculated, steric hindrance of ACE2 binding by the bulky IgM molecule were the primary mediator of increased neutralization (144), then mAbs that competed with the ACE-2-Fc chimera might have been predicted to display the greatest enhancement with multimerization. However, while mAbs 297 and 305 each competed with ACE2-Fc and exhibited similar sub-picomolar affinity to RBD and 15 ng/ml potency as IgG, multimerization as IgM effected 12- vs. 4-fold increases in activity, respectively. One explanation for variance in multimerization impact is differing ability to cross-link spike proteins/virions as assembled pentamers, a geometric or paratope property that would increase potency in neutralization assays but not be detected via techniques used to quantify binding. The limited impact of multimerization on clone 239, which binds at the RBD core, may be due relative steric hindrance for IgM in accessing the base of RBD, reducing the potential for cross-linking (145). While our studies are limited by reliance on competition assays rather than direct structural studies to define the RBD epitope, our combined findings suggest that the impact of multimerization is influenced by factors other than proximity to the ACE2 footprint.

In our study of MBC-derived mAbs targeting malaria merozoite surface proteins, enhanced avidity by multimerization as pentameric IgM or engineered hexameric IgG drove increased activity in parasite-blocking assays (58). Anti-SARS-CoV-2 mAbs with lower affinities for RBD

might therefore be predicted to benefit most from multimerization. Indeed, two of the lowest affinity clones, 203 and 207, showed the greatest benefit of multimerization (21-23 fold).

Although neutralization assays that use a spike pseudotyped lentivirus have been validated for IgG mAbs, differences between pseudovirus and true SARS-CoV-2 might impact the assessment of IgM/multimer activity. We therefore assessed one mAb pair using a live viral assay. The results for clone 297 IgG and IgM mAbs in a plaque assay that employed a SARS-CoV-2 isolate were nearly identical to the data generated using the pseudovirus neutralization assay (**Fig. 3.1 F**). In summary, multimerization as IgM increased potency across an unexpectedly broad range of target epitopes and affinities, including for mAbs that exhibited sub-picomolar affinity and potent neutralizing activity as IgG monomers.

3.2.2 *SARS-CoV-2-specific IgM$^+$ B cells encode BCRs that primarily bind RBD when expressed as IgM.*

Having shown that the activities of IgG$^+$ MBC-derived neutralizing antibodies are enhanced by expression as IgM, we next sought to investigate the characteristics of RBD-specific IgM$^+$ MBCs present in the same donors (81). We therefore determined BCR sequences from antigen-experienced RBD-specific IgM$^+$ B cells collected but not previously evaluated in our prior study (**Table 3.1**). BCRs from IgM-expressing cells with a classic MBC surface phenotype (CD21$^+$CD27$^+$) exhibited evidence of somatic mutation. The extent of mutation was less than observed in malaria-specific IgM$^+$ MBCs (54) likely reflecting the different kinetics of the immune responses to these pathogens, the time between exposure and sample collection, and/or the likelihood of multiple exposures in a malaria-endemic region (146). Of note, near-germline sequences can encode potent SARS-CoV-2 neutralizing antibodies (132,147,148). Consistent with data that the fraction of RBD-specific MBCs that are IgM$^+$ declines in the months following a first

infection in unvaccinated individuals, most IgM^+ MBC BCR sequences were isolated at early time points post-infection (81,85,149). While our data is limited by the duration of the study, other work suggests that individuals infected 12 mo. prior to analysis can retain long-lived IgM^+ MBCs (55,150).

To understand the potential contribution of IgM memory to the antibody pool, we built a library of plasmids from the antigen specificity-determining V(D)J sequences of each BCR. Heavy chains were cloned into alternative plasmids to allow us to directly compare the binding and functional properties when expressed as the native IgM isotype vs. as IgG. As an initial screen, we tested supernatants from cells co-transfected with a plasmid encoding the BCR-derived light-chain and a plasmid encoding its paired heavy chain variable region upstream of the gamma1 constant region (to make IgG), or the mu constant region (IgM). In this manner, 26 IgM-encoded BCRs were expressed as IgG and IgM antibodies. Despite achieving similar concentrations of IgG or IgM as assessed using anti-isotype ELISA, RBD binding was detected primarily for supernatants containing IgM (**Fig. 3.4**, **A** and **B).** Clones that bound RBD as IgM, but not IgG, likely represent low-affinity receptors that benefit from enhanced avidity provided by IgM's multimeric structure. Our results demonstrate the value of studying IgM BCRs as IgM antibodies and highlight the ability of tetramer-based enrichment to identify even very low-affinity antigen-specific MBCs (78). Notably, supernatant from cells producing an IgM antibody derived from clone 204 prevented RBD from binding to human ACE2, a surrogate for neutralization (**Fig. 3.4 C**) (151).

3.2.3 *A mAb derived from an IgM^+ MBC is a potent neutralizer of SARS-CoV-2.*

Next, we aimed to determine whether IgM BCR clone 204 encoded a neutralizing antibody. We therefore produced purified 204 IgG and IgM for use in advanced assays. To measure affinity, 204 IgG was immobilized onto sensor tips that were immersed into solutions with various

concentrations of RBD. Next, we immobilized RBD on a sensor and allowed varying dilutions of IgG or IgM antibody to bind, such that a calculated dissociation constant (Kd) reflected relative affinity, or avidity. For 204 IgG, the avidity assay Kd was 9.45 nM, while the 204 IgM Kd could not be calculated (**Fig. 3.4 D**). Consistent with our observations of malaria-specific multimerized antibodies, IgM strongly resisted dissociation through increased numbers of binding events and/or the effective increase in local concentration of binding moieties.

To assess neutralizing activity, we performed plaque reduction tests with SARS-CoV-2 and 204 IgM or IgG. 204 IgM, but not 204 IgG, exhibited potent neutralization (**Fig. 3.4**, **E** and **F**). In comparing the two isotypes, the NT-50 was 66-fold lower for 204 IgM than the clonally identical IgG. Thus, ~400-fold fewer molecules of IgM than IgG were required to achieve equivalent reduction in plaques vs. untreated controls (**Fig. 3.4 G**). Interestingly, while 204 IgG affinity and potency was lower than the IgG MBC-derived antibodies tested above, 204 IgM's observed neutralizing potency was similar to the highly potent 297 IgM. To investigate whether a unique target site explained the robust effect of multimerization for clone 204, we again performed competitive BLI assays with well-characterized mAbs and the IgG^+ MBC-derived mAbs (**Fig. 3.3 B** and **D, Fig. 3.4 H**). Adding 204 IgG did not increase sensor-detected RBD binding after immersions into solution containing IgG mAbs 284, 297, or 305, or the REGN10933 IgG and only moderately when 203 IgG or a LY-CoV555 Fab fragment was pre-loaded. Cumulatively, these results suggest that clone 204's RBD target site is similar to others in our panel and challenge the hypothesis that a unique epitope is responsible for the larger effect size of multimerization. Instead, our results support a model wherein the avidity benefit of IgM enables antibodies of mediocre affinity to achieve equivalent binding strength to a high-affinity interaction with lower valency. For clones with high baseline affinity, additional avidity may contribute less to enhanced function

than other attributes of IgM, such as the potential for crosslinking and greater steric hindrance for RBD:ACE2 interactions.

3.2.4 *IgM mAbs maintain neutralizing activity against variants that escape clonally identical IgG mAbs*

In settings of seasonal re-exposure to a highly variable pathogen, a likely future scenario for SARS-CoV-2, an ideal therapeutic, like an ideal humoral memory response, would tolerate mutations in neutralizing target sites, without incurring significant risk for autoreactivity. We hypothesized that IgM antibodies could accomplish this goal through enhanced avidity.

Based on observations that the Beta variant escapes neutralization by mAbs that are protective against earlier SARS-CoV-2 isolates, we compared binding to the Beta vs Wuhan-Hu-1 RBD for each IgG mAb by ELISA (84,149) (**Fig. 3.5 A**). In parallel, we also tested well-characterized IgG mAbs from each epitope-defined Class that are known to either exhibit limited (CR3022 and REGN10987), or substantial (C144 and C12.3) reductions in Beta vs Wuhan-Hu-1 RBD binding (87,138,152,153). Together with an ACE2-Fc chimera, the four published antibodies exhibited the predicted RBD binding profile, validating the RBD proteins generated for this assay and contextualizing results for our in-house mAbs. The parental MBCs in our study were isolated in early 2020, when a Wuhan-Hu-1-like virus (WA-1 SARS-CoV-2) predominated (146). Several IgG mAbs exhibited reduced binding to the Beta variant RBD protein, most notably 203 and 305. Next, affinity to Beta RBD was quantified using BLI for 203 IgG which exhibited significant loss of affinity in ELISA, and 297 IgG where binding appeared only slightly reduced (**Fig. 3.5 B**). The results were consistent with ELISAs: 16 nM to Beta vs. 4.4 nM to Wuhan-Hu-1 RBD for 203 IgG, and 6 nM to Beta vs. sub-picomolar to Wuhan-Hu-1 RBD for 297 IgG.

We next tested all nine IgG/IgM pairs for the ability to neutralize a Beta-spike pseudovirus. As expected, the poorest binders to Beta RBD failed to reduce pseudovirus infection as IgG mAbs, even at the highest concentration tested (2 μg/ml). In contrast, all IgM mAbs neutralized the WA-1 and Beta pseudoviruses with similar potencies (**Fig. 3.5 C**). These results expand on a study in which two IgM mAbs were tested for retained binding and neutralization activity against mutated RBD proteins and viruses (144). However, in this prior study, only 1 of the 2 IgM mAbs retained activity against the key mutations found in the Beta spike (NT-50 > 16 μg/ml). Our data contradict the authors' conclusion that careful selection of targeted epitope is necessary to identify antibodies that overcome escape mutations when multimerized as IgM. All IgM mAbs in our panel overcame even dramatic losses in neutralization potency. Besides testing more IgM/IgG pairs, our study differs in that MBC-encoded BCRs were the source for antigen-binding domains, while the previous work utilized variable regions derived from a phage display library and selected on the basis of binding to yeast-displayed protein. The ACE2-competing MBC-derived IgG mAbs are 10-fold more potent in neutralizing WA-1 SARS-CoV-2 than reported for the phage-derived IgG (144). These combined findings demonstrate that expression as IgM overcomes reduced affinity to the Beta variant for mAbs that target a range of RBD epitopes.

Next, we tested the previously unexplored question of whether IgM mAbs might also outperform clonally identical IgG against the Delta and Omicron BA.1 variants. In particular, the Omicron BA.1 variant is extensively mutated and partially or entirely escapes neutralization by all but one current Emergency Use Authorization mAb (154). Indeed, in neutralization assays using the Delta or Omicron BA.1 spike, 8 of the 9 IgG mAbs exhibited substantial reduction in activity (**Fig. 3.5**, **D** and **E**). In contrast, IgM mAbs retained activity at concentrations below 2 μg/ml. Apparent exceptions were against the Delta strain, for 203, 284, and 308.

Notably, 297 IgG acted as a broad neutralizer across all tested variants, with NT-50s for the Delta and Omicron BA.1 pseudoviruses of 111 ng/ml and 147 ng/ml respectively. Multimerization as IgM further improved potency to 23 ng/ml against both variants. To confirm that increased tolerance for spike mutations by IgM and broad neutralization by clone 297 were not specific to the pseudovirus, we next performed assays with true Delta SARS-CoV-2. As predicted, 297 IgG retained neutralizing activity, and multimerization as IgM enhanced potency 5-fold (**Fig. 3.5 F**).

3.2.5 *IgM mAbs exhibit enhanced protection in human airway cultures*

IgG antibodies do not easily penetrate the lung and respiratory epithelia, primary sites of SARS-CoV-2 infection. In contrast, pentameric IgM incorporates the J chain that allows transcytosis to mucosa (121,155). Evidence from subjects with immunoglobulin deficiencies suggests that IgM is important for long-term protection against respiratory pathogens (156). One potential challenge for an IgM therapeutic may be its reduced serum half-life relative to IgG (83). However, a recent study showed that an IgM mAb delivered to the nasal passages protected mice subsequently challenged with SARS-CoV-2 (144). To test the effect of IgM mAbs in human respiratory epithelia, we used polarized organotypic airway epithelia cultures generated from primary human bronchial epithelial cells (157) and applied SARS-CoV-2 together with either IgG or IgM mAbs. For 1 hour each subsequent day, the apical side of the culture was incubated with a small volume of mAb, and then rinsed (**Fig. 3.6 A**). Both the IgG and IgM antibodies reduced viral copy number in a dose-responsive manner (**Fig. 3.6**, **B** and **C**). Notably, a lower dose of IgM was required. As predicted by our experiments in cell lines, the enhanced performance of IgM was more striking for clone 204 than 297 due to the relatively lower potency of 204 IgG. These results demonstrate that

IgM mAbs are protective in a model that recapitulates physiologic conditions of the human airway, including air-exposure and mucus production.

Multimerization as the dimeric antibody isotype, IgA, has also been explored as a strategy to enhance SARS-CoV-2 neutralizing mAbs. Such reagents exhibit greater potency *in vitro* compared to clonally identical IgG, although not achieving that of IgM as demonstrated here or in other studies (84,144,158). IgA is more efficiently transported to respiratory mucosa, while IgM is maintained in higher concentrations in the blood, where it controls hematogenous spread, in addition to accessing the mucosa (83). Unlike IgA, IgM is a potent activator of complement, which both targets a pathogen directly and enhances the immune response. Delivery of IgM to respiratory mucosa might achieve both therapeutic effects (122). Interestingly, systemic delivery might offer enhanced stability of mAbs at the mucosal surface, as IgM acquires the protective secretory component during transcytosis (60).

Artificial multimers also harness avidity to enhance potency and/or breadth of SARS-CoV-2 binding domains. Among the most successful are trimeric nanobodies and a 24-valent structure of RBD-specific variable regions connected to an apoferritin scaffold (159–162). Interestingly, the hydrodynamic radius of the apoferritin construct is similar to IgM, potentially enabling similar cross-linking and steric hindrance (**Fig. 3.3 C**) (161). However, despite potent *in vitro* properties and proof of principle in small mammal models, novel proteins face greater challenges in safety, pharmacokinetics and anti-drug immune responses. Moreover, their function is likely limited to direct neutralization of virus. In contrast, IgM antibodies can interface with the endogenous immune system (83). Further, the use of variable domains derived from MBCs takes advantage of germinal center *in vivo* selection and refinement not feasible with phage display, including heavy- and light-chains that are selected in concert while, in parallel, screening against autoreactivity. Of

note, a recent report described three spike-specific mAbs presumed to be derived from IgM^+ MBCs (based on the dominant B cell subset present at the time of sample collection) (133). The two RBD-specific mAbs and one N-terminal domain-specific mAb exhibited increased neutralizing potency as IgM vs. IgG. However, expression of an IgG-derived, N-terminal domain-specific mAb as IgM did not statistically improve its activity. Our study expands upon these observations with characterization of > 20 RBD-specific mAbs derived from IgM^+ MBCs. Further, we provide a comprehensive assessment of the role of multimerization in enhancing neutralization and the impact of antibody isotype on resistance to viral escape.

The high per molecule potency and enhanced durability of binding across mutant viral proteins demonstrated here for IgM mAbs may help to explain the remarkable evolutionary conservation of multimeric IgM in jawed vertebrates (163). Although our investigation of IgM^+ MBCs encompassed a small number of cells, we identified a potent neutralizing antibody. These results contribute to growing evidence that IgM memory has an underappreciated role in protective immunity. IgM mAbs generated from diverse neutralizing antibodies are potent and broad neutralizers of SARS-CoV-2 and include candidate mAbs with likely therapeutic utility. Our results underscore the value of focused investigation into the role for IgM memory in immunity to SARS-CoV-2 and other evolving pathogens.

3.3 FIGURES

A

IgG:	Kd (nM):	NT-50 (ng/ml):
203	4.4	15
207	3.8	540
239	2.4	310
257	0.39	NP
284	6.2	5
297	sp	15
305	sp	15
308	0.16	NP

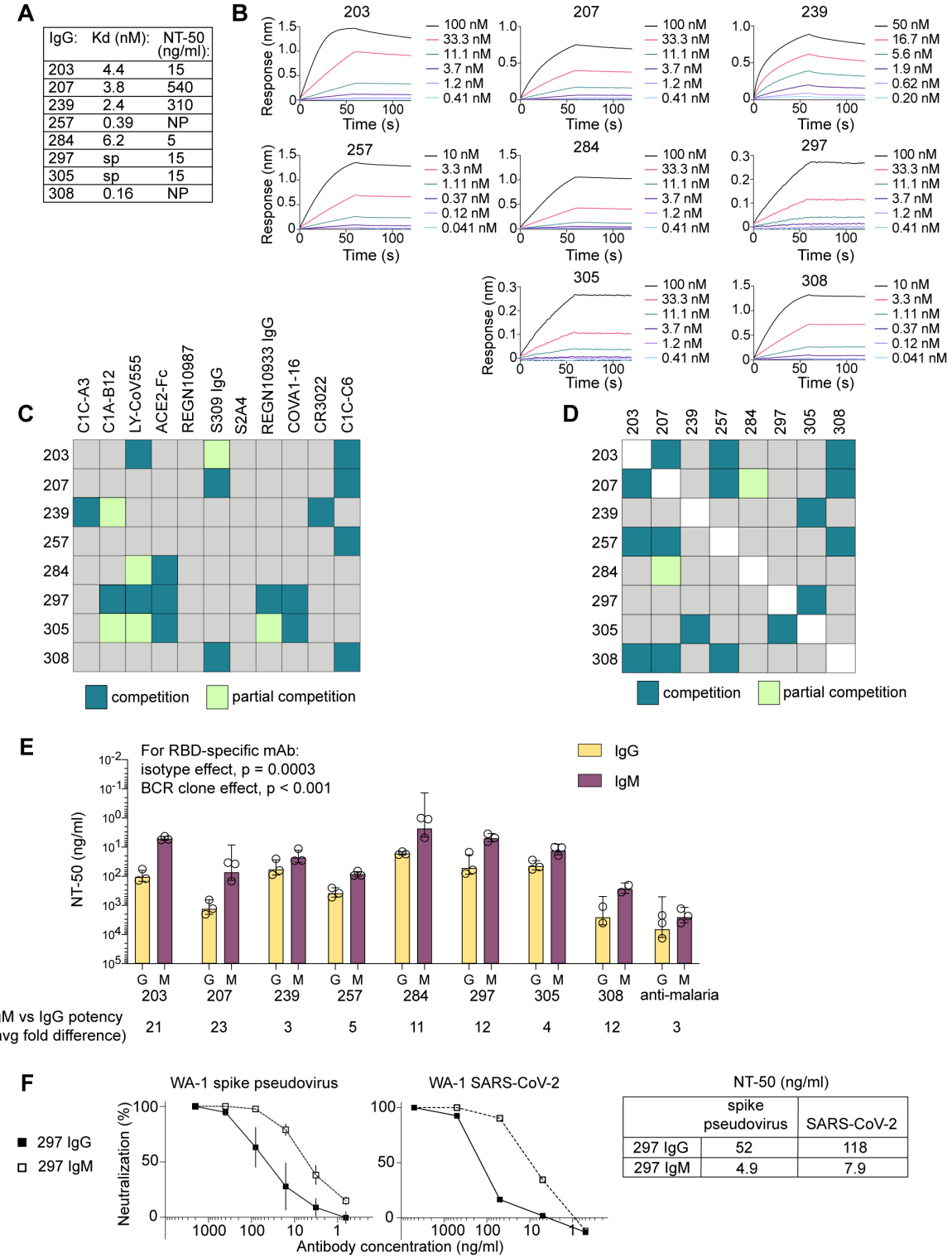

Figure 3.1. Diverse IgG$^+$ MBC-derived RBD-specific antibodies gain potency when expressed as IgM. (A) Panel of eight IgG$^+$ MBC-derived IgG mAbs indicating affinity for RBD

and NT50 of WA-1 SARS-CoV-2 in PRNT. (B) Binding kinetics for individual mAbs as determined by BLI using sensor-bound IgG mAbs and serial dilution of soluble RBD protein. Each mAb was tested with six dilutions of RBD. (C and D) Summary of epitope-mapping experiments showing relative competition for RBD between the indicated MBC-derived IgG and well-characterized Fabs (C) or each other (D); individual data are provided in Figs. 2.2 and 2.3 A. (E) Comparison of neutralizing potency of clonally identical IgG and IgM mAbs against pseudovirus. Bars indicate mean and SD for three independent experiments; individual symbols indicate the average of internal duplicates for each experiment. Average fold difference in NT50 potency for IgG vs. IgM for each BCR clone is shown below the graph. (F) Representative results for 297 IgM vs. IgG in neutralization assays using the pseudovirus (left panel; average and SD are shown for three independent experiments, each performed in duplicate) or a WA-1 SARS-CoV-2 PRNT (middle panel; representative of three independent experiments) and summary of NT50 data (right table).

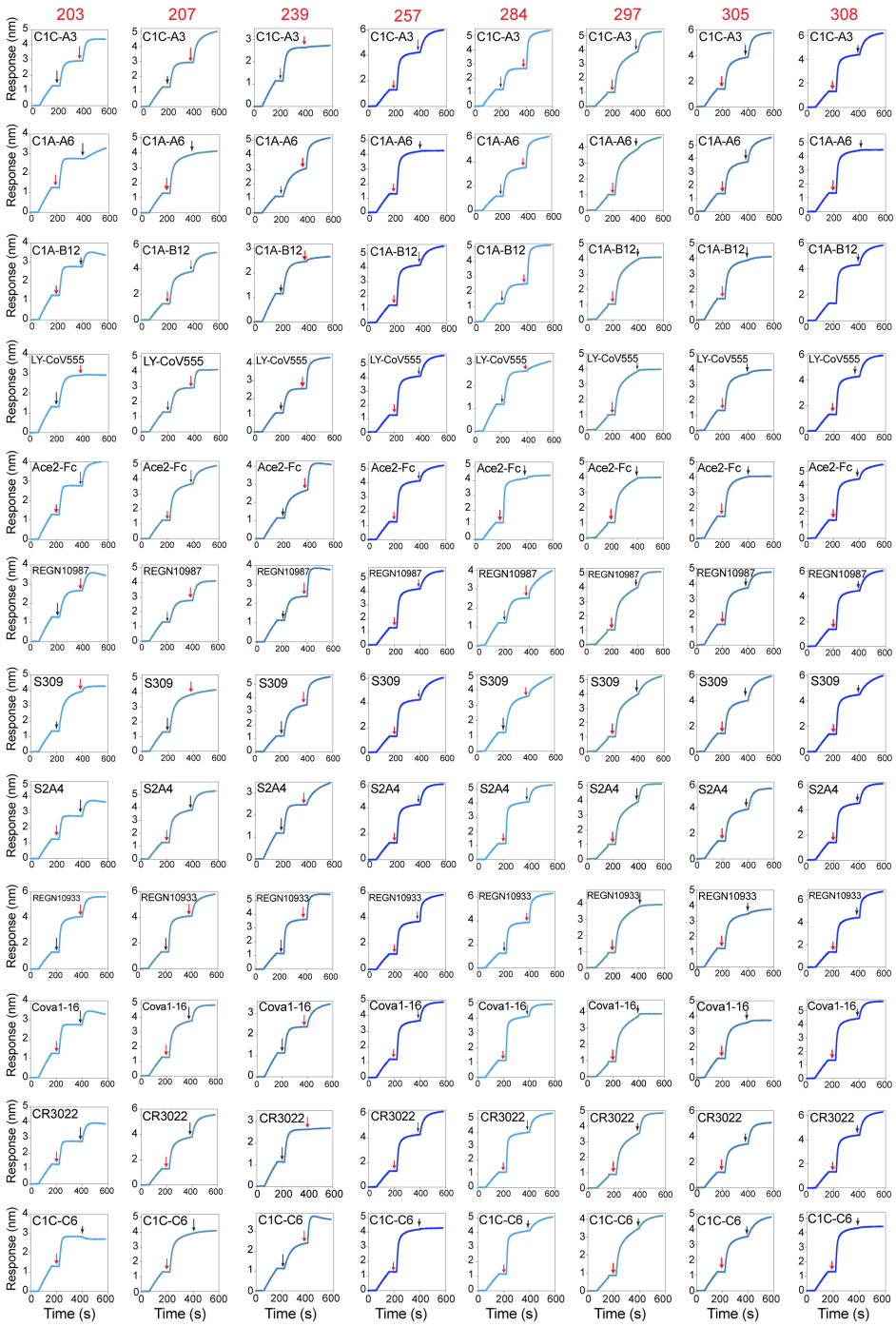

Figure 3.2. BLI competition assays. Competition with well-characterized mAbs for the panel of eight IgG+ MBC-derived IgG mAbs. The timing of the exposure to each antibody is indicated with a black arrow for the well-characterized mAb and a red arrow for the MBC-derived mAb.

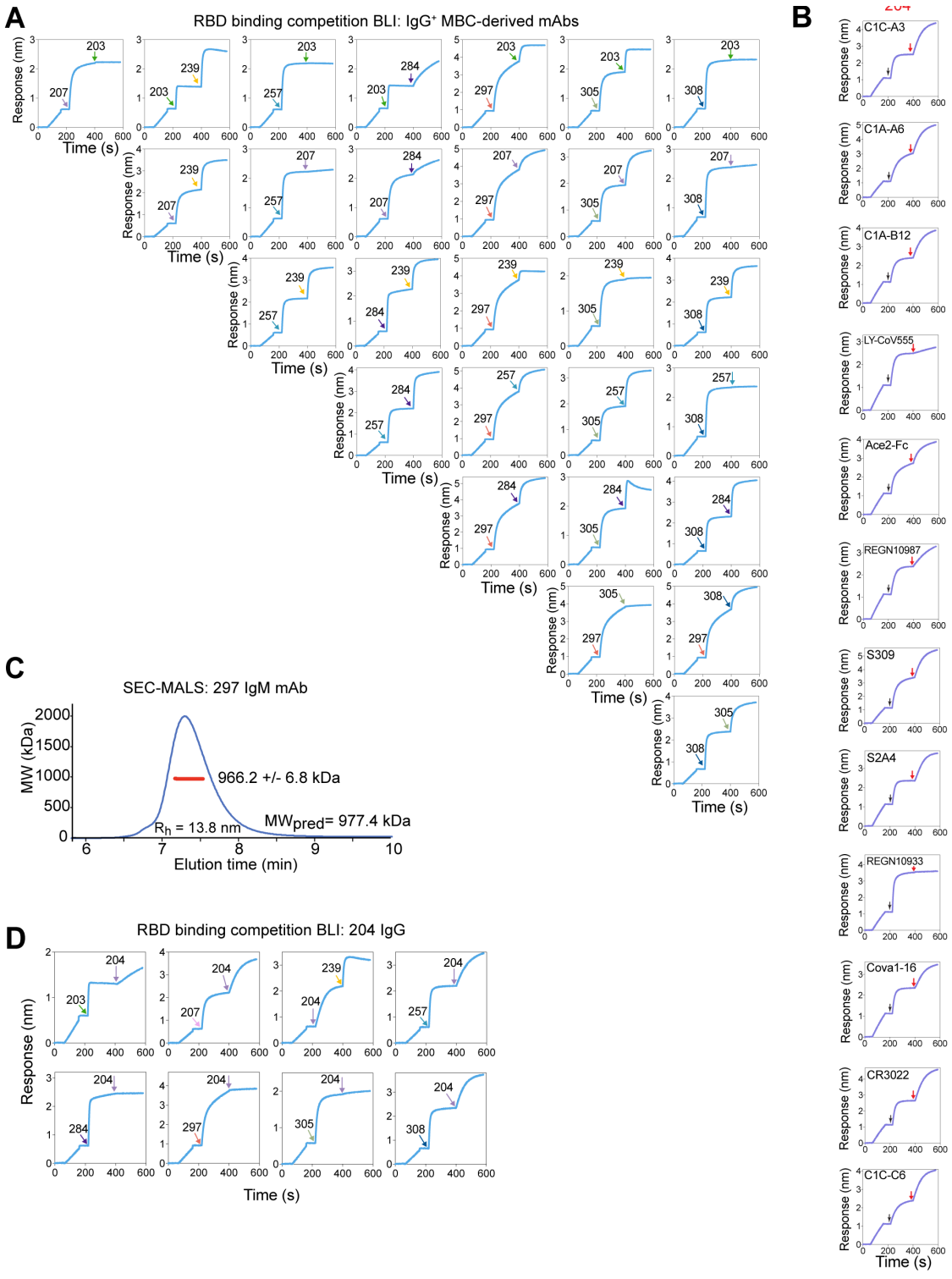

Figure 3.3. BLI competition assays and SEC-MALS demonstrating molecular weight of IgM pentamer. (A) Intrapanel competition BLI plots displaying sensor-detected RBD binding after addition of the indicated IgG$^+$ MBC-derived IgG mAb. (B) Competition with well-

characterized mAbs and the IgM^+ MBC^- derived 204 IgG mAb for RBD by BLI. (C) SEC-MALS traces for the purified 297 IgM mAb. The light scattering trace is in blue, and the molecular weight (MW) calculated from the combination of scattering, refractive index, and UV absorbance is shown in red across the peak elution window. The average calculated MW is shown in the inset, along with the predicted MW (MWpred). The error is based on the SD from the 56 scans along the peak elution profile; however, the expected uncertainty can be as large as 10% due to assumptions about molar extinction coefficients and glycan occupancy. The hydrodynamic radius (Rh) was estimated from dynamic light scattering, which was also measured online and indicated under the peak. (D) Competition of mAb 204 against the panel of eight IgG+ MBC-derived mAbs.

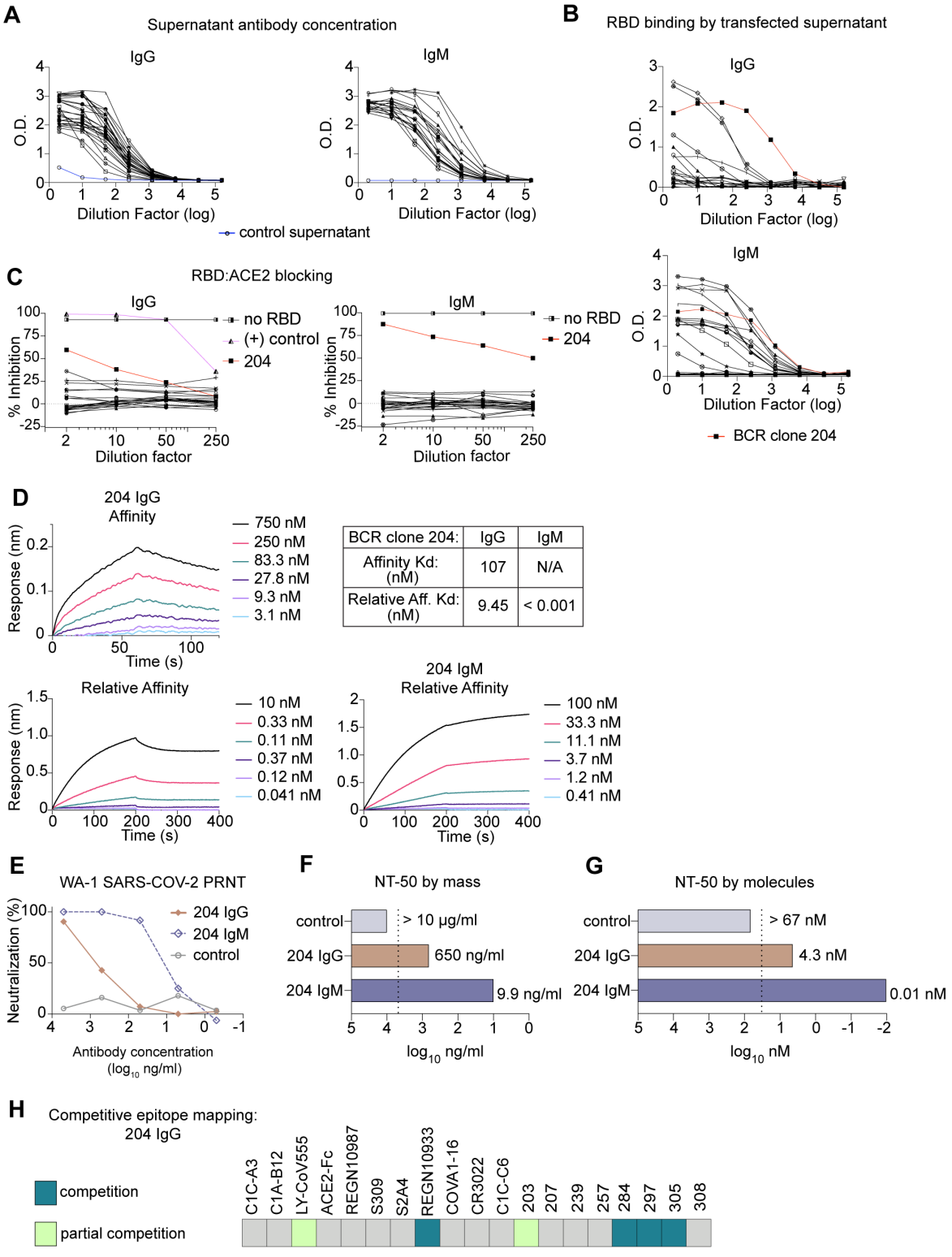

Figure 3.4. IgM memory B cells encode RBD-specific antibodies, including a neutralizing mAb with improved activity when expressed as IgM vs IgG. Supernatants from cells

transfected with plasmids encoding IgM+ MBC-derived mAbs as IgG vs. IgM screened by ELISA for: A) anti-IgG (left) or -IgM (right), with untransfected supernatant as a negative control (blue); or B) binding to SARS-CoV-2 spike RBD protein. (C) Supernatants' ability to block RBD from binding to plate-bound human ACE2. BCR clone #204 is highlighted (in red) in B and C. IgG+ MBC-derived antibody, 297 IgG, is included as a positive control (in pink) in C. Data is representative of 2 independent experiments performed in triplicate. (D) Biolayer interferometry data showing binding and dissociation kinetics of BCR clone #204 as purified IgG vs. IgM. (E) SARS-CoV-2 PRNT on Vero cells at the indicated concentrations of 204 IgG vs. IgM, or an anti-malaria mAb (negative control, Thouvenel et al., 2021). NT-50 titers are shown based on mass (F) or molar (G) concentrations. For conditions that did not approach an NT-50, an arbitrary NT-50 was assigned of 2X the maximum concentration tested (dashed line). Assay was performed in duplicate and repeated at least twice. (H) Epitope mapping of mAb 204 IgG by BLI against well characterized Fabs/mAbs and the other mAbs in our panel; individual data are provided in Fig. 3.3 B and D.

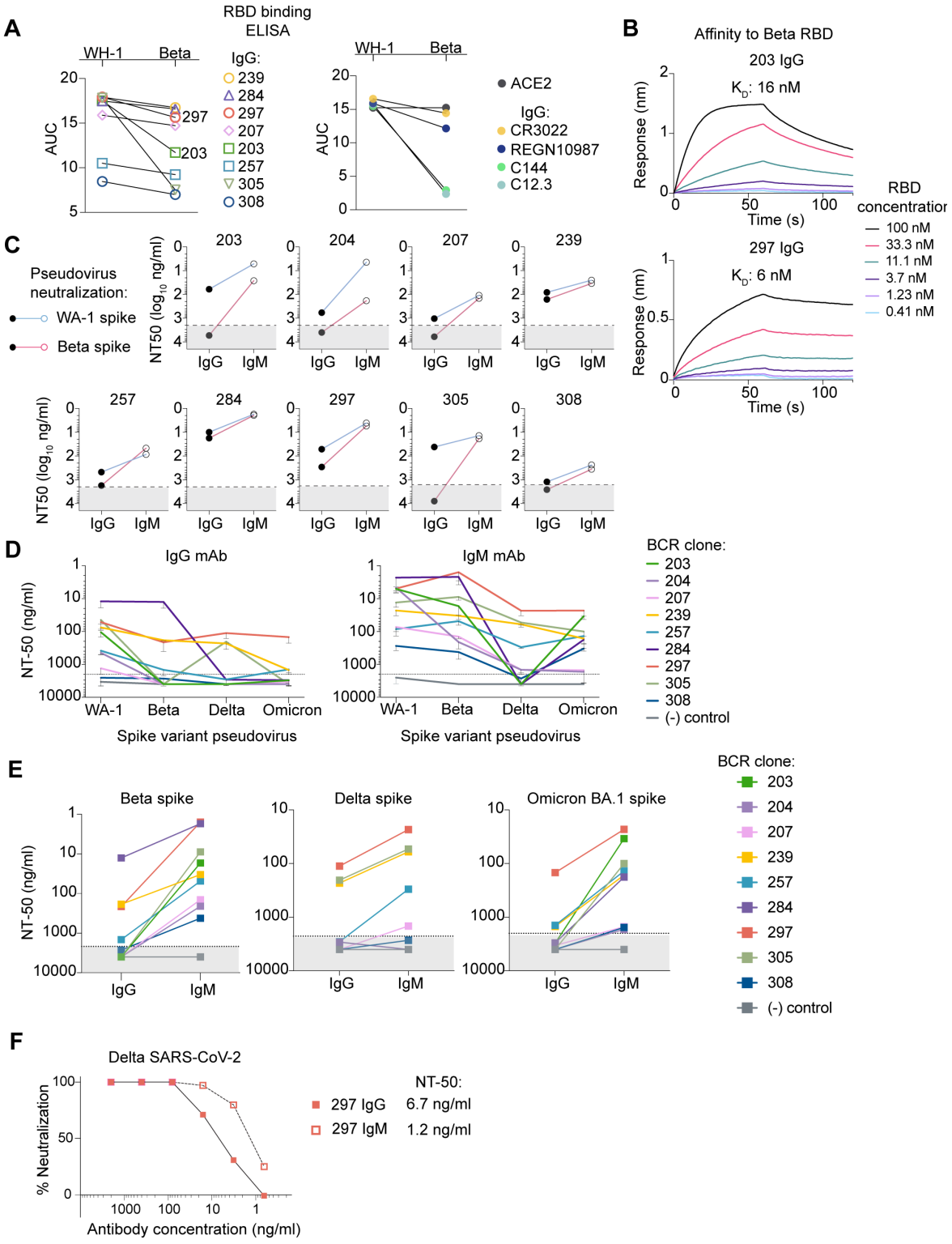

Figure 3.5 IgM antibodies retain activity against viral spike variants that escape clonally identical IgG. A) Binding to Wuhan-Hu-1 (WH-1) or Beta variant RBD proteins by purified

IgG mAbs in ELISAs, quantified as the area under the curve (AUC) for a 10 dilution series. Results for the panel of eight IgG^+ MBC-derived mAbs are shown (left panel). For clarity, simultaneously performed ELISAs testing well-characterized IgG mAbs, or an ACE2-Fc fusion protein (ACE2), are shown separately (right). Data is representative of 2 independent experiments performed in triplicate. (B) Affinity for Beta RBD of representative antibodies with significantly reduced binding, 203 (top), and moderate reduced binding, 297 (bottom). (C) Neutralization potencies for each mAb as IgG vs IgM against WA-1 (blue) or Beta (pink) spike pseudovirus. Dashed line illustrates the maximum antibody concentration tested (2 μg/ml). For antibodies that did not approach an NT-50, the NT-50 is graphed arbitrarily in the shaded area as 4 μg/ml. Each IgG/IgM pair was tested in duplicate against both viruses in 3 independent experiments. (D) Varying neutralization potency against WA-1, Beta, Delta, and Omicron BA.1 spike pseudoviruses for IgG (left) vs IgM (right) mAbs. Error bars illustrate mean +/- SD for $\geq$ 3 experiments with internal duplicates. (E) Summary neutralization potencies of IgG vs. IgM mAbs for the indicated variants in experiments described in D. Control: malaria-specific IgG or IgM (MaliA01 mAbs, Thouvenel et al., 2021). (F) Neutralization in a Vero cell plaque reduction assay of Delta SARS-CoV-2 for 297 IgG vs. IgM. Representative plot of 5 independent experiments.

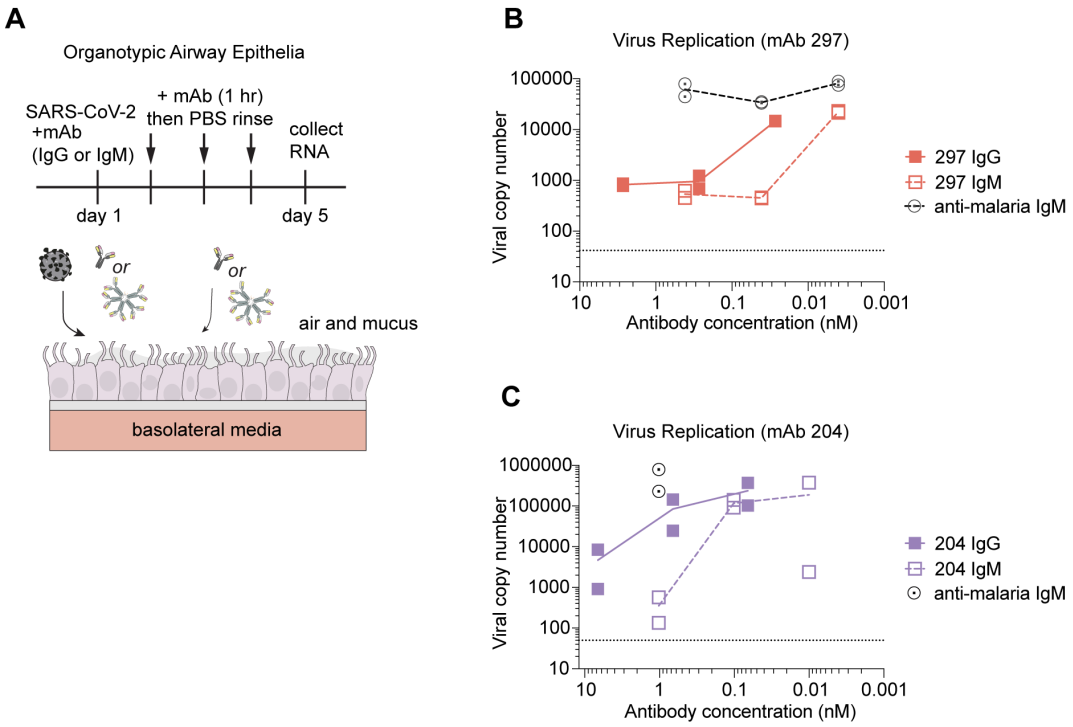

Figure 3.6. An anti-RBD IgM mAb protects against SARS-CoV-2 infection in differentiated human airway epithelia cultures. A) Schematic of experimental design using airway epithelial cultures differentiated to an organotypic state at an air-liquid interface (ALI). (B-C) Quantification of viral RNA copy number in ALI cultures treated with the indicated antibody. B and C represent independent experiments and used cultures generated from primary human bronchial epithelial cells derived from unique donors. Each condition was tested in independent duplicates. For B, duplicates were pooled as RNA prior to qPCR.

Table 3.1. Characteristics of singly-sorted RBD-specific IgM$^+$ B cells from which BCRs were cloned and tested

	Phenotype	Clone	Subject	Day	Heavy Chain (HC)	Light Chain (LC)	Germline HC (%)	Germline LC (%)	Heavy Chain Junction Sequence
●	CD21$^+$CD27$^+$	200	165	42	IGHV 1-8	IGLV 1-44	100	99.3	CARGPGCTSLTCPYYFDYW
■	CD21$^+$CD27$^+$	204	165	42	IGHV 3-48	IGKV 3-11	98.3	100	CARALRYSSSWVDYW
▲	CD21$^+$CD27$^+$	208	165	42	IGHV 5-51	IGLV 2-14	97.2	96.2	CARLWGSPGNYYYAMDVW
□	CD21$^+$CD27$^+$	219	165	42	IGHV 3-23	IGLV 2-18	96.5	99.7	CAKDHLYASSSAFDYW
▼	CD21$^+$CD27$^+$	213	165	42	IGHV 1-8	IGLV 1-44	98.6	97.5	CARGPGCSSLNCPYFFDYW
◆	CD21$^+$CD27$^+$	214	165	42	IGHV 5-51	IGLV 1-44	96.9	96.8	CARHLPSFGDYSPYFDYW
○	CD21$^-$CD27$^+$	215	165	42	IGHV 5-51	IGLV 2-14	98.3	97.9	CARLWGSPANYYYGMDVW
△	CD21$^+$CD27$^+$	221b	165	42	IGHV 3-74	IGKV 1-5	100	99.3	CARGRVGDW
◇	CD21$^+$CD27$^+$	222	165	42	IGHV 5-51	IGLV 2-14	97.2	96.2	CARLWGSPGNYYYAMDVW
✳	CD21$^+$CD27$^+$	223	165	42	IGHV 5-51	IGLV 2-14	98.3	98.3	CARLWGSPANYYYGMDVW
★	CD21$^+$CD27$^+$	224	165	42	IGHV 1-8	IGLV 1-44	99.3	99.0	CARGPGCTSTSCPYYFDYW
+	CD21$^+$CD27$^+$	226	165	42	IGHV 5-51	IGLV 2-14	96.2	98.3	CARLWGSPENYYYGMDVW
×	CD21$^+$CD27$^+$	226b	165	42	IGHV 5-51	IGLV 2-23	96.2	99.7	CARLWGSPENYYYGMDVW
♀	CD21$^-$CD27$^+$	261	165	42	IGHV 1-8	IGLV 1-44	97.9	97.6	CARGPGCSSLNCPYFFDYW
⊡	CD21$^-$CD27$^-$	237	165	42	IGHV 3-21	IGLV 3-21	100	100	CARDPDSSSSLFDYW
ı	CD21$^+$CD27$^+$	266	165	42	IGHV 5-51	IGLV 2-14	100	98.6	CARLWGSPGNYYYGMDVW
⊙	CD21$^+$CD27$^+$	230	165	42	IGHV 3-9	IGLV 2-14	100	98.6	CAKDIEYGYGKYYFDYW
⊗	CD21$^+$CD27$^-$	240	164	30	IGHV 3-33	IGLV 3-19	100	98.9	CARLTGGSSWEHFDYW
I	CD21$^+$CD27$^-$	271	164	30	IGHV 3-7	IGLV 6-57	100	100	CASAPYYYGAFDIW
⊠	CD21$^+$CD27$^-$	242b	164	30	IGHV 1-2	IGLV 2-14	100	98.6	CARQADIAAAGTGDWFDPW
❁	CD21$^+$CD27$^+$	243	169	34	IGHV 4-39	IGLV 2-23	100	100	CARRVRYNYGHYFDYW
♂	CD21$^-$CD27$^-$	244	169	34	IGHV 5-51	IGKV 2-29	100	99.7	CARHIPHYSSSWYGAGDYW
○	NA	282	165	89	IGHV 1-2	IGKV 4-1	100	100	CARDQGWGPPMWLLQFDPW
◓	NA	295	165	89	IGHV 3-72	IGKV 2-28	100	100	CARGPYCSSTSCYYYYGMDVW
◒	CD21$^+$CD27$^+$	304	165	89	IGHV 5-51	IGLV 2-14	97.6	98.3	CARVWGSPANYYYGLDVW
◐	NA	310	169	73	IGHV 4-31	IGKV 3-11	100	100	CAREGVVPAANGAYYYYGMDVW

3.4 Materials and Methods

Memory B cell isolation

Peripheral blood samples from convalescent COVID-19 subjects were obtained with informed consent under the approval of the University of Washington Institutional Review Board (Gale Lab, IRB 00009810) and isolated as previously described (81). Briefly, PBMC were thawed, washed and stained with a decoy tetramer and then a RBD tetramer, magnetically enriched (Miltenyi Biotec) and bound cells were stained with surface antibodies. Single tetramer-positive B cells were index sorted using a FACS Aria II and collected in 96 well plates containing SMART-Seq v4 capture buffer (Takara Bio) for BCR sequencing.

BCR sequencing and cloning

Our methods for BCR sequencing of singly-sorted B cells are previously described (81). Briefly, following cDNA amplification using SMART-Seq v4 (Takara Bio) at half reaction volume, BCR sequences from each cell's cDNA were amplified in a multiplex reaction using a universal 5' primer for the template switch region combined with pooled 3' primers for the mu, gamma, alpha, kappa, and lambda constant regions. After gel electrophoresis to confirm amplification, amplicons were purified and sequenced by Sanger sequencing (Genbank IDs: ON886550-ON886835). Alignment of trimmed sequences was performed using IGMT/HighV-QUEST (118). Primer design and cloning into expression vectors followed the manufacturer's protocol for In-Fusion Cloning (Takara Bio). Each light chain was cloned into vectors of its respective isotype, kappa or lambda. All heavy chains were cloned into IgG1 plasmids. Additionally, heavy chains from BCR clones 203, 207, 239, 257, 284, 297, 305, 308 (81), and any

heavy chain cDNA sequence using mu constant regions were also cloned into IgM plasmids. Cloned plasmids were sequenced and screened to ensure concordance with the parental cDNA.

Production of purified mAbs

Production of purified IgG and IgM mAbs was carried out by polyethylenemine transfection of heavy- and light-chain plasmids as previously described (58), except that a plasmid encoding human J chain (Genbank ID: NM_144646.4) was included in IgM transfections at a mu:light:J chain plasmid ratio of 1:1:1, and supernatant was collected at days 3 and 6 following transfection. After 0.4 μm filtration, antibody purification was carried out following manufacturer's instructions using a HiTrap Protein G HP purification column for IgG antibodies (GE Healthcare), and a POROS CaptureSelect IgM Affinity Matrix Column (Thermo Fisher Scientific) for IgM. Antibodies were concentrated and buffer-exchanged to PBS at 1-3 mg/ml using Amicon Ultra Centrifugal filters (MilliporeSigma) and then filter-sterilized and stored at -80°C. Antibody concentration and purity were assessed by spectrophotometry and protein gel electrophoresis.

SEC-MALS

SEC-MALS was performed using an Agilent 1260 HPLC system coupled to a light scattering detector (miniDawn Treos, Wyatt Instruments) and a refractive index detector (TRex, Wyatt Instruments). 50 μL of each IgM construct (1 mg/ml) were injected and flowed over a Sepax SRTC SEC column (5 μm, 300Å, 4.6 x 300 mm with a 4.6 x 50 mm matching guard column) at a flow rate of 0.35 mL/min in 150 mM sodium phosphate pH 7.0, 0.02% sodium azide. Chromatograms were aligned, integrated, and the MW calculated using ASTRA (Wyatt

Instruments). A refractive index of 0.181 was used for calculations reflecting a weighted combined contribution of protein 0.185 and glycan 0.146 (164). A glycan content of 8635 Da of N-linked glycans on each heavy chain and 2155 Da for the J-chain was based on the estimated average of the predominant glycoforms observed in previous site-specific glycan studies of human IgM (165).

ELISA for antibody expression and RBD binding

Cloned heavy- and light-chain plasmids derived from RBD-specific IgM^+ B cells were initially screened in small scale transfections. 293T cells (ATCC) were plated at 80% confluence and transfected with 0.5 μg each of paired heavy and light chain plasmids using polyethylenimine. Sixteen hours later media was replaced with serum free-media and after 3-4 days supernatants were harvested and cellular debris was removed by centrifugation. Antibody expression levels were determined using Human IgG or Human IgM ELISA Antibody Pair Kit (Stemcell Technologies) according to the manufacturer's instructions. RBD-specificity was determined by ELISA as previously described (81). Briefly, 96-well high bind plates (Corning) were coated with 2 μg/ml SARS-CoV-2 RBD protein overnight at 4°C, washed with PBS and 0.05% Tween 20 (PBS-T), blocked with 3% milk in PBS-T and incubated with serially diluted culture supernatants for 2 h at room temperature. Plates were washed and bound antibodies were detected using anti-human IgG-HRP or anti-human IgM-HRP (Jackson ImmunoResearch) at a 1:3000 dilution followed by 1X 3,3',5, 5"-Tetramethylbenzidine (Invitrogen) and 1M HCl. Optical density was measured on a spectrophotometer at 450 and 570 nm and data was analyzed in Prism (GraphPad).

ACE2:RBD blocking surrogate virus neutralization test (SVNT)

Antibody ability to inhibit interaction with human ACE2 were assessed at previously described (151). 96 well plates (Corning) were coated with 5 μg/ml hACE2-Fc in 100mM carbonate buffer overnight at 4°C. Plates were washed with PBS-T, blocked with 3% milk in PBS-T. Monoclonal antibodies were serially diluted and incubated with 18 ng of SARS-CoV2 RBD-HRP for 1 h at 37°C then added to the blocked plates for 1 h at RT. Binding was detected using TMB, reactions quenched with 1M HCL and absorbance was measured at 450 and 570 nm. Percent inhibition was calculated as (1- SampleO.D./NegativeControlO.D.) x 100 and analyzed in Prism (GraphPad).

Biolayer interferometry (BLI)

BLI assays for affinity and relative affinity/avidity were performed ambient temperature with shaking set at 1000 rpm using an Octet Red 96 System (Pall FortéBio/Sartorius). Individual IgG mAbs (for affinity assays), or purified RBD protein (for relative affinity/avidity assays), were diluted 10 μg/mL to in Kinetics buffer (1x HEPES-EP+ (Pall FortéBio), 0.05% nonfat milk, and 0.02% sodium azide). Biosensors were hydrated in Kinetics buffer for 10 minutes, and then the diluted protein was immobilized onto Protein A biosensors (IgG mAbs in affinity assays) or anti-Penta-His biosensors (RBD in avidity assays), and then equilibrated in Kinetics buffer for 60 s. For affinity assays, monomeric RBD was diluted to 5000 nM, 750 nM, or 100 nM in Kinetics buffer and serially diluted three-fold for a final concentration of 20.6 nM, 3.1 nM, and 0.4 nM respectively. For avidity assays, individual IgG or IgM mAbs were diluted to 100 nM or 10 nM in Kinetics buffer and serially diluted three-fold for a final concentration of 0.41 nM or 0.041 nM respectively in a black 96-well Greiner Bio-one microplate at 200 μL per well. To measure association, loaded biosensors were dipped into the diluted protein. Association and

dissociation was performed for 60 s each in affinity assays. Association and dissociation times for avidity assays were extended to 200 s each. The data were baseline subtracted and the plotted using the Pall FortéBio/Sartorius analysis software (version 12.0).

Protein production for biolayer interferometry competition assays

For BLI competition assays, we produced SARS-CoV-2 spike protein RBD (GenBank ID: QHD43416.1 residues 319-541), as previously described (141). Previously characterized antibodies were produced as either IgGs or Fabs for use in this assay. Antibodies REGN10933 and REGN10987 (40), CR3022 (140), C1A-B12, C1C-A3, C1C-C6, and C1A-A6 were prepared and purified as previously described (152). Antibodies S309, LY-CoV555, Cova1-16, and S2A4 were also generated as previously described (141). An Fc-fusion protein comprising the human ACE2 ectodomain (GenBank ID: BAB40370.1 residues 18-740) was expressed and purified as previously described (152).

Biolayer interferometry competition assays

We performed competition experiments using an Octet RED 96e (Sartorius). First, we loaded SARS-CoV-2 spike protein RBD onto streptavidin sensors (FortéBio) at 1.5 μg ml^{-1} for 80 s in kinetic buffer [PBS containing 0.02% (v/v) Tween and 0.1% (v/v) BSA]. For each pair of antibodies tested, we associated the first antibody (IgG, Fab, or ACE2-Fc fusion protein) at 250 nM for 180 s. We then associated the second analyte (IgG, Fab, or ACE2-Fc fusion protein) at 250 nM for 180 s. All antibodies were tested as Fabs unless only the IgG form was available. Antibodies tested as Fabs include 203, C1A-B12, C1C-A3, C1C-C6, Cova1-16, CR3022, LY-CoV555, REGN10987, and S2A4. Antibodies tested as IgGs include 204, 207, 239, 257, 284, 297,

305, 308, C1A-A6, S309, and REGN10933. We used FortéBio data analysis software and Prism (v9.0.1) (GraphPad) to generate and analyze curves for competition assays. Antibodies were designated to be competing if there was little to no change in the refractive index following association of the second protein.

Production of spike-variant pseudoviruses

To make Beta and Omicron BA.1 spike pseudotyping plasmids, sequence fragments encoding the variant spike protein were gene synthesized (Integrated DNA Technologies, Coralville, IA) and cloned into a digested plasmid (NR-53765; BEI Resources, NIAID, NIH) using NEBuilder HiFi DNA Assembly (NEB, Ipswitch, MA). To produce pseudotyped virus, 293T cells were transiently transfected with a vector plasmid encoding luciferase (NR-52516, BEI Resources), a pseudotyping plasmid encoding the Beta, Omicron BA.1, WA-1 (gift from David Veesler, University of Washington), or Delta (pLV-Spike-V8, InvivoGen, San Diego, CA) spike, and a psPAX2 helper plasmid (Genscript). Forty-eight hours after transfection, culture supernatant was harvested and passed through a 0.22 μm filter. 100X concentrations of virus were achieved by overnight centrifugation at 8,500 x g at 4°C, and then resuspending the pellet in Hank's balanced salt solution.

Pseudovirus neutralization assays

Pseudovirus neutralization assays were performed as previously described (143,166). Briefly, ACE-2 expressing 293T cells (BEI Resources: NR-52511) were seeded onto poly-L-lysine coated 96 well-plates and grown to 85-95% confluency. Pseudovirus was incubated with serially diluted IgG or IgM mAbs, or media alone, for 1 h at 37°C and then gently applied to cells. At 48

hours post-infection, cells were lysed following manufacturer's instructions using the Bright-Glo Luciferase Assay System reagent (E2610, Promega), and luminescence was measured in black-bottom plates using a Centro LB Microplate Luminometer (Berthold Technologies) with MikroWin 2000 software set to a 1 s exposure time. Percent neutralization was calculated relative to the luminescence in control wells that had been transduced with virus co-incubated with media alone (internal for each plate, average of 6 wells), after subtracting background luminescence in virus-exposed 293T cells that lacked ACE2 expression (internal for each plate, average of 6 wells). NT-50 was calculated by sigmoidal interpolation method in Prism (Graphpad). If a curve could not be fit and 50% neutralization was not achieved at any dilution, where necessary for the purposes of data visualization, an arbitrary NT-50 was assigned at 2 x the highest dilution tested.

Plaque reduction neutralization test (PRNT)

Plaque reduction neutralization tests were performed as previously described (81,167). Briefly, purified mAbs were diluted 1:10 followed by serial dilution. Diluted mAbs were mixed 1:1 with 600 PFU/ml SARS-CoV-2 WA-1 or Delta (BEI Resources; NR-52881 and NR-55612) virus in PBS+0.3% cold water fish skin gelatin (Sigma) and incubated for 30 min at 37 °C. Next, the mAb/virus mixture, or virus-only and mAb only control solutions, was applied to duplicate wells of Vero cells in a 12 well-plate and incubated for 1 h at 37 °C, rocking every 15 minutes. Following incubation, plates were washed with PBS and overlaid with a 1:1 mixture of 2.4% Avicel RC-591 (FMC) and 2X MEM (Thermo Fisher Scientific) supplemented with 4% heat-inactivated FBS and Penicillin/Streptomycin (Thermo Fisher Scientific). The overlay was removed 2 days after infection, plates were fixed by applying 10% formaldehyde (Sigma-Alrdich) in PBS and incubating for 30 min at room temperature, and stained in a solution of 1% crystal

violet (Sigma-Aldrich) in 20% ethanol (Thermo Fisher Scientific). Percent neutralization was calculated as (1 – # sample plaques/# positive control plaques) x 100. Data was analyzed in Prism (GraphPad) and an NT-50 for each condition was calculated by sigmoidal interpolation.

Air-liquid interface primary airway epithelial cultures

Airway epithelial cultures were differentiated to an organotypic state at an air-liquid interface (ALI) as previously described (157). Briefly, bronchial epithelial cells were obtained under study #12490 approved by the Seattle Children's Institutional Review Board and following the rules of the Declaration of Helsinki of 1975. Cells were differentiated for 21 days at an ALI on 12-well collagen-coated Corning® plates with permeable transwells in PneumaCult ALI media (Stemcell). SARS-CoV-2 WA-01 was added to the apical surface of differentiated cultures at an MOI of 0.5 together with either IgG or IgM mAbs for 1 hour then removed. Every 24 hours mAb in 100 μL of PBS was again added to the apical surface of cultures for 1 hour then removed. After 96 hours of infection RNA was extracted from cultures and SARS-CoV-2 replication was assessed by measuring viral genome copy number by quantitative PCR, with duplicate assays of harvested RNA from each SARS-CoV-2-infected experimental condition completed (Genesig Coronavirus Strain 2019-nCoV Advanced PCR Kit, Primerdesign).

Author Contributions

Conceptualization: M. Hale, J. Netland, Y. Chen, C.D. Thouvenel, M. Pepper and D.J. Rawlings. Supervision/direction: N.P. King, M. Guttman, M. Gale Jr, J. Abraham, J.S. Debley, M. Pepper and D.J. Rawlings. Funding acquisition: N.P. King, M. Guttman, J. Abraham, J.S. Debley, M. Pepper and D.J. Rawlings. Investigation: M. Hale, J. Netland, Y. Chen, C.D. Thouvenel, K.N.

Smith, L.M. Rich, E.R. Vanderwall, M.C. Miranda, J. Eggenberger, L. Hao, M.J. Watson, C.C. Mundorff and L.B. Rodda. Data analysis: M. Hale, J. Netland, Y. Chen, C.D. Thouvenel, K.N. Smith, L.M. Rich, E.R. Vanderwall, M.C. Miranda, J. Eggenberger, L. Hao, M.J. Watson, C.C. Mundorff, L.B. Rodda, M. Guttman, J. Abraham, J.S. Debley, M. Pepper and D.J. Rawlings. Writing - original draft: M. Hale. Writing - review and editing: M. Hale, J. Netland, K.N. Smith, M. Guttman, J. Abraham, J.S. Debley, M. Pepper and D.J. Rawlings.

Chapter 4. Summary and Future Directions

4.1 IgM MEMORY HAS A ROLE IN IMMUNE PROTECTION FROM DIVERSE PATHOGENS

4.1.1 *MBCs that recognize an important P. aeruginosa virulence factor are present in patients with cystic fibrosis.*

Using a novel tetramer reagent, we found increased numbers of PcrV-specific B cells in individuals with CF compared to healthy blood donors among the general population. Employing new, efficient methods for single-cell BCR sequencing, we then obtained hundreds of sequences from *P. aeruginosa*-specific B cells in 3 donors with CF. Intriguingly, only small numbers of somatically hypermutated PcrV-specific MBCs could be isolated in the two chronically infected donors, while the donor who had clinically cleared their infection had abundant somatically-hypermutated MBCs of IgG, IgM and IgA isotypes. Additional work will be required to clarify to what extent differences in the circulating PcrV-specific B cell populations drive or reflect relative bacterial clearance in these donors. Many *P. aeruginosa* isolates in chronically-infected adults have been found to have reduced expression of genes associated with toxin secretion (168), although a subset of isolates retain expression of PcrV (169). The extent to which loss of the toxin secretion system is mediated by a targeted immune response *vs.* bacterial adaptation or quorum sensing is not clear. The nature and fate of PcrV-specific B cells in chronically-infected individuals clearly warrants further study. Meanwhile, better understanding of the PcrV-specific B cells in those who have achieved clinical clearance could inform the development of a successful vaccine. We did not pursue fuller B cell phenotyping in this early study, opting to focus instead on the

generation of novel mAbs. The reagents (PcrV tetramer) and methods (optimized next-generation single cell sequencing) we developed here have begun to facilitate other work by our group that will more rigorously survey PcrV-specific B cells in CF.

4.1.2 *IgM MBCs in COVID-19 convalescent subjects encode neutralizing antibodies against SARS-CoV-2.*

We performed the first targeted study of IgM memory B cells arising following mild COVID-19 illness. Further distinguishing our work, we studied IgM MBC-encoded antibodies via expression as pentameric IgM, rather than as the isotype generally employed for convenience, monomeric IgG. Among 26 sequenced IgM MBCs, we discovered an IgM MBC that encoded a highly potent neutralizing IgM mAb, suggesting that IgM MBCs could contribute to a rapid neutralizing response upon re-exposure to SARS-CoV-2. When considered with our data that IgM mAbs had broader cross-neutralizing activity than IgG mAbs with the same variable regions, our findings support a model in which IgM MBCs seed the secondary immune response with avidly binding antibodies that are advantageous in protection from evolving pathogens.

Although not explored here, mucosal IgM MBCs are a wholly untapped source of potential therapeutic mAb sequences against respiratory pathogens, one potential future direction for this project. Mucosal IgM B cells are an important but incompletely understood component of mucosal immunity in humans, best studied in the context of the gut. Secretory IgM and IgA target partially over-lapping but non-redundant microbe species to protect the epithelial barrier and preserve commensal tolerance in humans (170,171). Consistent with a role as a keystone of mucosal humoral immunity, gut resident IgM MBCs are clonally related to IgA MBCs, as well as IgM- and IgA-secreting plasma cells (57) and asymptomatic IgA deficiency is associated with a compensatory increase in IgM in adulthood that protects from enteropathy (170,172). Future work

could explore the BCR repertoires of pathogen-specific resident IgA and IgM MBCs in airway mucosa, and determine the protective efficacy of mAbs derived from these sequences.

4.2 MBC BCR SEQUENCING WILL ENABLE EFFICIENT DISCOVERY AND OPTIMIZATION OF HUMAN MABS WITH CLINICALLY-RELEVANT PROTECTIVE ACTIVITY AGAINST IMPORTANT HUMAN PATHOGENS.

4.2.1 *Protective anti-P. aeruginosa mAbs can be generated using sequences found in cystic fibrosis B cells.*

We cloned and expressed 20 BCRs from PcrV-specific CF B cells in two donors as IgG and/or IgM mAbs. Our original intention was to focus on MBCs as source cells for novel mAbs. However, donor 1, who was chronically infected by *P. aeruginosa*, had very limited PcrV-specific $CD21^{+}CD27^{+}$ MBCs. Surprisingly, in this donor we nevertheless identified a germline BCR that encoded a very high affinity mAb, CF 411. We also identified a second germline BCR, CF 408, that bound PcrV well as an IgM mAb and moderately as IgG. Finally, we expressed a near-germline mAb that exhibited efficient binding to PcrV.

For initial *in vivo* experiments, we opted to first test the two germline mAbs, as IgG, the most widely used mAb isotype. Based on results of the *in vitro* binding assay, we predicted that CF 411 would outperform CF 408. When given intranasally, both CF 408 and CF 411 significantly reduced lung bacterial load. As both achieved several log reductions in bacterial load when compared to an off-target mAb, we did not detect efficacy differences for the apparent moderate and high-affinity anti-PcrV mAbs. Groups developing mouse-derived mAbs have similarly found that relative *in vitro* activity did not always predict *in vivo* efficacy (101). Most strikingly, our

human CF-derived mAbs conferred protection that matched an IgG mAb that replicates the PcrV-binding component of gremubamab.

With these encouraging results, we proceeded to isolate and sequence PcrV-specific B cells from a second donor. Donor 2 had numerous PcrV-specific MBCs. Using an optimized sequencing pipeline, we rapidly obtained paired chain sequences for cloning that resulted in additional, novel PcrV-specific mAbs, now with definitive MBC origins. *In vivo* studies of the most promising MBC-derived mAbs are now underway. Given the excellent results of our experiments with CF 408 and 411, additional studies (*eg.* titration to even lower doses) may be required to test the hypothesis that MBC-derived mAbs provide superior protection, and to select the best candidates for continued pre-clinical development for the treatment or prevention of *P. aeruginosa* infection in vulnerable populations.

Although the robust protection offered by our germline mAbs was initially surprising to us, it is not unreasonable to imagine that germline BCRs might be selected for given the long co-evolution between humans and bacterial species (173,174). *P. aeruginosa* pre-dates the dawn of microbiological culture techniques. Carle Gessard, adapting Pasteur's methods, grew the first isolate from soldier's linen bandages in 1882, in "neutralized urine and carrot extract" (175). A gram-negative bacteria for which historical data is more readily available, *Yersinia pestis*, of greater interest to genomic archeologists as the causative agent of the Black Death pandemic, is now believed to date back to the Stone Age (174). LcrV, a component of the *Y. pestis* toxin-injecting machinery, is closely homologous to PcrV. Mice immunized with either protein form cross-protective antibodies (111). Therefore, immune gene selection pressure from historical and pre-historic plague pandemics (173) might also have impacted the anti-pseudomonal immune response.

The federal government is almost certainly the largest purchaser of anti-infectious mAbs (15,176), and funds their development and manufacturing optimization through challenge grants (177). Although plague is now a rare disease, it is more common than anthrax infection, for which two commercial mAbs (obiltoxaximab and raxibacumab) are now maintained in government stockpiles (176). Like *B. anthracis*, *Y. pestis* is categorized by the CDC as a category A potential bioweapon agent. Therefore, a reasonable, parallel direction for future work on human anti-PcrV mAbs could be to include preliminary tests of candidates' activity also against *Y. pestis*, *eg.* by screening *in vitro* for binding to LcrV. Although purely speculative, our findings comparing anti-SARS-CoV-2 IgM *vs.* IgG mAbs hint that an anti-PcrV IgM mAb might be more likely to achieve protective efficacy against dual pathogens (103).

4.2.2 *Multimerization as IgM enhances the neutralizing activity of mAbs against diverse SARS-CoV-2 variants.*

We had predicted that pentameric IgM mAbs would exhibit greater per molecule and per mass neutralizing potency of SARS-CoV-2 based on our prior findings for multimerized mAbs that targeted the blood stage of malarial infections (58). Using a similar approach of generating paired IgG and IgM mAbs that differed only in the constant regions, we now demonstrated that IgM mAbs are indeed more potent neutralizers of SARS-CoV-2 than IgG mAbs with the same specificity and binding domains. Importantly, we also showed that multimerization as IgM enhanced activity for human MBC-derived mAbs with a range of affinities and epitopes within RBD. Moreover, multimerization as IgM enabled mAbs to neutralize mutated virus variants that escaped identical IgG mAbs.

Within these experiments, we also identified an MBC-derived mAb (mAb 297) that neutralized all tested pseudovirus variants in our study, even as IgG. Collaborator groups have

since validated that mAb 297 is indeed broadly neutralizing against true SARS-CoV-2 (178). Although retaining activity against Omicron BA.1 and 2, mAb 297 IgG did lose activity against Omicron BA.3 and 4 (178). Our own work suggests that 297 IgM could have retained even broader activity.

Thanks to broader population immunity, as well as the the challenges encountered for IgG mAbs with escape mutants, commercial appetite for anti-SARS-CoV-2 mAbs is lower today than at the height of our studies (15). However, in addition to our own studies in malaria, recent publications by others hint at growing interest in IgM mAbs targeting other infectious diseases. For example, neutralization of Zika virus in mice by an IgM mAb derived from a previously-infected subject was reported in the months following initial publication of our own data for SARS-CoV-2 (103,179). Although the isolation strategy employed did not reveal surface phenotype, the source cell was identified on the basis of sequencing as a somatically hypermutated IgM-expressing B cell. Consistent with our findings for SARS-CoV-2 neutralizing mAbs, the Zika-specific IgM mAb exhibited reduced neutralizing activity when expressed as IgG (179).

4.3 CONCLUDING REMARKS

The outbreak of the COVID-19 pandemic, which coincided with the start of my dedicated period for graduate study, provoked an unprecedented intensity in global efforts to develop new therapeutics, including mAbs. Even the President of the United States was receiving experimental mAb infusions (15). Antibody treatments' promise and the challenge of ensuring safety, efficacy and access were on unprecedented public display.

Patients who receive mAbs for chronic diseases like Crohn's disease or familial hypercholesterolemia require monthly infusions or injections that can be burdensome (17,32). Our hope is that highly potent mAbs targeting respiratory pathogens could be used as adjunctive treatments in acutely ill, hospitalized patients, where treatment half-life and logistics are of less relative importance. However, certain vulnerable populations, for example people with cystic fibrosis or non-CF bronchiectasis, might benefit from prophylactic use, similarly to the use of palivizumab as RSV prophylaxis in pre-term infants (21). In these situations, the reduced serum half-life of IgM mAbs relative to IgG make the potential increased cost and inconvenience more problematic (83). Direct delivery to the airway is one potential solution (144). Modifications of the Fc region or J chain that would extend serum half-life by enabling FcRn recognition are also being attempted (180). In addition, the manufacturing process must be refined to improve commercial feasibility and lower cost to patients (83). An intriguing option that could bypass low serum half-life and antibody production challenges would be to ensure sustained, long-term delivery by means of an engineered, long-lived plasma cell (181,182). As anti-drug immune responses are still of concern, the use of fully human mAbs would be especially appropriate in a long-term cell therapy. We hope that our work generating human mAbs from well-defined MBCs in previously-infected subjects will expand available treatment options for challenging diseases, while in parallel contributing to vaccine development via increased understanding of protective immunity. For patients who are intrinsically or pharmaceutically immune-compromised, or where high-efficacy vaccines are unavailable or have low socio-cultural acceptability, we anticipate a continued value for optimizing passive immunity with enhanced anti-pathogen mAbs.

FUNDING

This work was supported in part by: Seattle Children's Research Integration Hub Covid-19 Award (to D.J. Rawlings), Cystic Fibrosis Foundation Grant to M. Pepper, Burroughs Wellcome Fund Pilot Grant (to J. Abraham and M. Pepper), the Bill & Melinda Gates Foundation grants OPP1156262 (to N.P. King) and OPP1126258 (M. Guttman), Burroughs Wellcome Fund Career Award for Medical Scientists (J. Abraham), and National Institutes of Health grants T32GM007266 (M. Hale), T32GM007753 (K.N. Smith), R01AI153191 (M. Guttman), R01AI163160 (J. Debley), and K24AI150991-01S1 (J. Debley), the Cystic Fibrosis Research and Translation Center (R.L. Gibson and S. McNamara), and the Tom Hansen Investigator for Pediatric Innovation Endowment at Seattle Children's (D.J. Rawlings).

REFERENCES

1. World Health Organization. A visualized overview of global and regional trends in the leading causes of death and disability 2000-2019 [Internet]. [cited 2023 Jun 2]. Available from: https://www.who.int/data/stories/leading-causes-of-death-and-disability-2000-2019-a-visual-summary

2. Theuretzbacher U, Outterson K, Engel A, Karlén A. The global preclinical antibacterial pipeline. Nat Rev Microbiol. 2020 May;18(5):275–85.

3. Lofano G, Gorman MJ, Yousif AS, Yu WH, Fox JM, Dugast AS, et al. Antigen-specific antibody Fc glycosylation enhances humoral immunity via the recruitment of complement. Science Immunology. 2018 Aug 17;3(26).

4. Cooper MD, Alder MN. The Evolution of Adaptive Immune Systems. Cell. 2006 Feb 24;124(4):815–22.

5. Ripperger TJ, Bhattacharya D. Transcriptional and Metabolic Control of Memory B Cells and Plasma Cells. Annu Rev Immunol. 2021 Apr 26;39(1):345–68.

6. Sela-Culang I, Kunik V, Ofran Y. The Structural Basis of Antibody-Antigen Recognition. Frontiers in Immunology. 2013;4.

7. Kober C, Manni S, Wolff S, Barnes T, Mukherjee S, Vogel T, et al. IgG3 and IgM Identified as Key to SARS-CoV-2 Neutralization in Convalescent Plasma Pools. PLOS ONE. 2022 Jan 4;17(1):e0262162.

8. Moticka EJ. Chapter 3 - Two Effector Mechanisms of the Adaptive Immune Response. In: Moticka EJ, editor. A Historical Perspective on Evidence-Based Immunology [Internet]. Amsterdam: Elsevier; 2016. p. 21–9. Available from: https://www.sciencedirect.com/science/article/pii/B9780123983817000034

9. Czajkowsky DM, Shao Z. The human IgM pentamer is a mushroom-shaped molecule with a flexural bias. PNAS. 2009 Sep 1;106(35):14960–5.

10. Phan TG, Grigorova I, Okada T, Cyster JG. Subcapsular encounter and complement-dependent transport of immune complexes by lymph node B cells. Nat Immunol. 2007 Sep;8(9):992–1000.

11. Diebolder CA, Beurskens FJ, de Jong RN, Koning RI, Strumane K, Lindorfer MA, et al. Complement Is Activated by IgG Hexamers Assembled at the Cell Surface. Science. 2014 Mar 14;343(6176):1260–3.

12. Pyzik M, Sand KMK, Hubbard JJ, Andersen JT, Sandlie I, Blumberg RS. The Neonatal Fc Receptor (FcRn): A Misnomer? Frontiers in Immunology. 2019;10:1540.

13. Arce Vargas F, Furness AJS, Litchfield K, Joshi K, Rosenthal R, Ghorani E, et al. Fc Effector Function Contributes to the Activity of Human Anti-CTLA-4 Antibodies. Cancer Cell. 2018 Apr 9;33(4):649-663.e4.

14. Zhang W, Gordon M, Schultheis AM, Yang DY, Nagashima F, Azuma M, et al. FCGR2A and FCGR3A Polymorphisms Associated With Clinical Outcome of Epidermal Growth Factor Receptor–Expressing Metastatic Colorectal Cancer Patients Treated With Single-Agent Cetuximab. JCO. 2007 Aug 20;25(24):3712–8.

15. Strohl WR, Ku Z, An Z, Carroll SF, Keyt BA, Strohl LM. Passive Immunotherapy Against SARS-CoV-2: From Plasma-Based Therapy to Single Potent Antibodies in the Race to Stay Ahead of the Variants. BioDrugs. 2022 May 1;36(3):231–323.

16. Tuft L, Ramsdell SG. The antibody response in the human being after injection with normal horse serum. J Exp Med. 1929 Sep 30;50(4):431–7.

17. Lu RM, Hwang YC, Liu IJ, Lee CC, Tsai HZ, Li HJ, et al. Development of therapeutic antibodies for the treatment of diseases. Journal of Biomedical Science. 2020 Jan 2;27(1):1.

18. Greig SL. Obiltoxaximab: First Global Approval. Drugs. 2016 May;76(7):823–30.

19. Mulangu S, Dodd LE, Davey RT, Tshiani Mbaya O, Proschan M, Mukadi D, et al. A Randomized, Controlled Trial of Ebola Virus Disease Therapeutics. N Engl J Med. 2019 Dec 12;381(24):2293–303.

20. Lee A. Ansuvimab: First Approval. Drugs. 2021;81(5):595–8.

21. Garegnani L, Styrmisdóttir L, Roson Rodriguez P, Escobar Liquitay CM, Esteban I, Franco JV. Palivizumab for preventing severe respiratory syncytial virus (RSV) infection in children. Cochrane Database Syst Rev. 2021 Nov 16;11(11):CD013757.

22. Beccari MV, Mogle BT, Sidman EF, Mastro KA, Asiago-Reddy E, Kufel WD. Ibalizumab, a Novel Monoclonal Antibody for the Management of Multidrug-Resistant HIV-1 Infection. Antimicrob Agents Chemother. 2019 May 23;63(6):e00110-19.

23. Melsheimer R, Geldhof A, Apaolaza I, Schaible T. Remicade® (infliximab): 20 years of contributions to science and medicine. Biologics. 2019 Jul 30;13:139–78.

24. Knight DM, Trinh H, Le J, Siegel S, Shealy D, McDonough M, et al. Construction and initial characterization of a mouse-human chimeric anti-TNF antibody. Mol Immunol. 1993 Nov;30(16):1443–53.

25. The PREVAIL II Writing Group. A Randomized, Controlled Trial of ZMapp for Ebola Virus Infection. N Engl J Med. 2016 Oct 13;375(15):1448–56.

26. Qiu X, Alimonti JB, Melito PL, Fernando L, Ströher U, Jones SM. Characterization of Zaire ebolavirus glycoprotein-specific monoclonal antibodies. Clinical Immunology. 2011 Nov 1;141(2):218–27.

27. Pedrioli A, Oxenius A. Single B cell technologies for monoclonal antibody discovery. Trends in Immunology. 2021 Dec 1;42(12):1143–58.

28. Wang Z, Wang G, Lu H, Li H, Tang M, Tong A. Development of therapeutic antibodies for the treatment of diseases. Mol Biomed. 2022 Nov 22;3:35.

29. Horspool AM, Sen-Kilic E, Malkowski AC, Breslow SL, Mateu-Borras M, Hudson MS, et al. Development of an anti-Pseudomonas aeruginosa therapeutic monoclonal antibody WVDC-5244. Front Cell Infect Microbiol. 2023 Apr 14;13:1117844.

30. Waldron JL, Schworer SA, Kwan M. Hypersensitivity and Immune-related Adverse Events in Biologic Therapy. Clin Rev Allergy Immunol. 2022 Jun;62(3):413–31.

31. Wincup C, Dunn N, Ruetsch-Chelli C, Manouchehrinia A, Kharlamova N, Naja M, et al. Anti-rituximab antibodies demonstrate neutralizing capacity, associate with lower circulating drug levels and earlier relapse in lupus. Rheumatology. 2022 Nov 12;keac608.

32. Vaisman-Mentesh A, Gutierrez-Gonzalez M, DeKosky BJ, Wine Y. The Molecular Mechanisms That Underlie the Immune Biology of Anti-drug Antibody Formation Following Treatment With Monoclonal Antibodies. Front Immunol. 2020 Aug 18;11:1951.

33. Scott CT. Mice with a human touch. Nat Biotechnol. 2007 Oct 1;25(10):1075–7.

34. Patnaik A, Kang SP, Rasco D, Papadopoulos KP, Elassaiss-Schaap J, Beeram M, et al. Phase I Study of Pembrolizumab (MK-3475; Anti–PD-1 Monoclonal Antibody) in Patients with Advanced Solid Tumors. Clinical Cancer Research. 2015 Sep 30;21(19):4286–93.

35. Programme on International Nonproprietary Names (INN), Quality Assurance and Safety: Medicines (QSM). General policies for monoclonal antibodies [Internet]. World Health Organization; 2009 [cited 2023 May 24]. Available from: https://web.archive.org/web/20100601233746/http://www.who.int/medicines/services/inn/Generalpoliciesformonoclonalantibodies2009.pdf

36. Strand V, Balsa A, Al-Saleh J, Barile-Fabris L, Horiuchi T, Takeuchi T, et al. Immunogenicity of Biologics in Chronic Inflammatory Diseases: A Systematic Review. BioDrugs. 2017 Aug 1;31(4):299–316.

37. Castillo J, Milani C, Mendez-Allwood D. Ofatumumab, a second-generation anti-CD20 monoclonal antibody, for the treatment of lymphoproliferative and autoimmune disorders. Expert Opinion on Investigational Drugs. 2009 Apr 1;18(4):491–500.

38. Mazumdar S, Greenwald D. Golimumab. MAbs. 2009;1(5):422–31.

39. DiGiandomenico A, Keller AE, Gao C, Rainey GJ, Warrener P, Camara MM, et al. A multifunctional bispecific antibody protects against Pseudomonas aeruginosa. Science Translational Medicine. 2014 Nov 12;6(262):262ra155-262ra155.

40. Hansen J, Baum A, Pascal KE, Russo V, Giordano S, Wloga E, et al. Studies in humanized mice and convalescent humans yield a SARS-CoV-2 antibody cocktail. Science. 2020 Aug 21;369(6506):1010–4.

41. McCafferty J, Griffiths AD, Winter G, Chiswell DJ. Phage antibodies: filamentous phage displaying antibody variable domains. Nature. 1990 Dec 6;348(6301):552–4.

42. Jespers LS, Roberts A, Mahler SM, Winter G, Hoogenboom HR. Guiding the selection of human antibodies from phage display repertoires to a single epitope of an antigen. Biotechnology (N Y). 1994 Sep;12(9):899–903.

43. Brekke OH, Sandlie I. Therapeutic antibodies for human diseases at the dawn of the twenty-first century. Nat Rev Drug Discov. 2003 Jan;2(1):52–62.

44. Baker KP, Edwards BM, Main SH, Choi GH, Wager RE, Halpern WG, et al. Generation and characterization of LymphoStat-B, a human monoclonal antibody that antagonizes the bioactivities of B lymphocyte stimulator. Arthritis & Rheumatism. 2003;48(11):3253–65.

45. Shin W, Lee HT, Lim H, Lee SH, Son JY, Lee JU, et al. BAFF-neutralizing interaction of belimumab related to its therapeutic efficacy for treating systemic lupus erythematosus. Nat Commun. 2018 Mar 23;9(1):1–11.

46. Ferrara F, Erasmus MF, D'Angelo S, Leal-Lopes C, Teixeira AA, Choudhary A, et al. A pandemic-enabled comparison of discovery platforms demonstrates a naïve antibody library can match the best immune-sourced antibodies. Nat Commun. 2022 Jan 24;13(1):1–12.

47. Xiang R, Wang Y, Wang L, Deng X, Huo S, Jiang S, et al. Neutralizing monoclonal antibodies against highly pathogenic coronaviruses. Curr Opin Virol. 2022 Apr 1;53:101199.

48. Cancro MP, Tomayko MM. Memory B cells and plasma cells: The differentiative continuum of humoral immunity. Immunological Reviews. 2021;303(1):72–82.

49. Kim W, Zhou JQ, Horvath SC, Schmitz AJ, Sturtz AJ, Lei T, et al. Germinal centre-driven maturation of B cell response to mRNA vaccination. Nature. 2022 Apr;604(7904):141–5.

50. Zhang Z, Mateus J, Coelho CH, Dan JM, Moderbacher CR, Gálvez RI, et al. Humoral and cellular immune memory to four COVID-19 vaccines. Cell. 2022 Jul 7;185(14):2434-2451.e17.

51. Weisel F, Shlomchik M. Memory B Cells of Mice and Humans. Annual Review of Immunology. 2017;35(1):255–84.

52. Lee JH, Sutton HJ, Cottrell CA, Phung I, Ozorowski G, Sewall LM, et al. Long-primed germinal centres with enduring affinity maturation and clonal migration. Nature. 2022 Sep;609(7929):998–1004.

53. Braddom AE, Bol S, Gonzales SJ, Reyes RA, Musinguzi K, Nankya F, et al. B Cell Receptor Repertoire Analysis in Malaria-Naive and Malaria-Experienced Individuals Reveals Unique Characteristics of Atypical Memory B Cells. Blader IJ, editor. mSphere. 2021 Oct 27;6(5):e00726-21.

54. Krishnamurty AT, Thouvenel CD, Portugal S, Keitany GJ, Kim KS, Holder A, et al. Somatically Hypermutated Plasmodium-Specific IgM+ Memory B Cells Are Rapid, Plastic, Early Responders upon Malaria Rechallenge. Immunity. 2016 Aug 16;45(2):402–14.

55. Viant C, Wirthmiller T, ElTanbouly MA, Chen ST, Cipolla M, Ramos V, et al. Germinal center–dependent and –independent memory B cells produced throughout the immune response. J Exp Med. 2021 Jun 9;218(8).

56. Pape KA, Taylor JJ, Maul RW, Gearhart PJ, Jenkins MK. Different B cell populations mediate early and late memory during an endogenous immune response. Science. 2011 Mar 4;331(6021):1203–7.

57. Magri G, Comerma L, Pybus M, Sintes J, Lligé D, Segura-Garzón D, et al. Human Secretory IgM Emerges from Plasma Cells Clonally Related to Gut Memory B Cells and Targets Highly Diverse Commensals. Immunity. 2017 Jul 18;47(1):118-134.e8.

58. Thouvenel CD, Fontana MF, Netland J, Krishnamurty AT, Takehara KK, Chen Y, et al. Multimeric antibodies from antigen-specific human IgM+ memory B cells restrict Plasmodium parasites. J Exp Med. 2021 Apr 5;218(4):e20200942.

59. Gasser R, Cloutier M, Prévost J, Fink C, Ducas É, Ding S, et al. Major role of IgM in the neutralizing activity of convalescent plasma against SARS-CoV-2. Cell Reports. 2021 Mar 2;34(9):108790.

60. Michaud E, Mastrandrea C, Rochereau N, Paul S. Human Secretory IgM: An Elusive Player in Mucosal Immunity. Trends in Immunology. 2020 Feb 1;41(2):141–56.

61. Velounias RL, Tull TJ. Human B-cell subset identification and changes in inflammatory diseases. Clin Exp Immunol. 2023 Jan 7;210(3):201–16.

62. Laidlaw BJ, Cyster JG. Transcriptional regulation of memory B cell differentiation. Nat Rev Immunol. 2021;21(4):209–20.

63. Zurbuchen Y, Michler J, Taeschler P, Adamo S, Cervia C, Raeber ME, et al. Human memory B cells show plasticity and adopt multiple fates upon recall response to SARS-CoV-2. Nat Immunol. 2023 Apr 27;24:955–65.

64. Shlomchik MJ. Do Memory B Cells Form Secondary Germinal Centers?: Yes and No. Cold Spring Harb Perspect Biol. 2018 Jan;10(1):a029405.

65. Xu Q, Milanez-Almeida P, Martins AJ, Radtke AJ, Hoehn KB, Oguz C, et al. Adaptive immune responses to SARS-CoV-2 persist in the pharyngeal lymphoid tissue of children. Nat Immunol. 2023 Jan;24(1):186–99.

66. Corti D, Misasi J, Mulangu S, Stanley DA, Kanekiyo M, Wollen S, et al. Protective monotherapy against lethal Ebola virus infection by a potently neutralizing antibody. Science. 2016 Mar 18;351(6279):1339–42.

67. Tsai DY, Wang CH, Schiro PG, Chen N, Tseng JY. Tracking B Cell Memory to SARS-CoV-2 Using Rare Cell Analysis System. Vaccines (Basel). 2023 Mar 26;11(4):735.

68. Leyendeckers H, Odendahl M, Löhndorf A, Irsch J, Spangfort M, Miltenyi S, et al. Correlation analysis between frequencies of circulating antigen-specific IgG-bearing memory B cells and serum titers of antigen-specific IgG. Eur J Immunol. 1999;29(4):1406–17.

69. Sapparapu G, Fernandez E, Kose N, Bin Cao, Fox JM, Bombardi RG, et al. Neutralizing human antibodies prevent Zika virus replication and fetal disease in mice. Nature. 2016 Dec;540(7633):443–7.

70. Kisalu NK, Idris AH, Weidle C, Flores-Garcia Y, Flynn BJ, Sack BK, et al. A human monoclonal antibody prevents malaria infection by targeting a new site of vulnerability on the parasite. Nat Med. 2018 May;24(4):408–16.

71. Kayentao K, Ongoiba A, Preston AC, Healy SA, Doumbo S, Doumtabe D, et al. Safety and Efficacy of a Monoclonal Antibody against Malaria in Mali. New England Journal of Medicine. 2022 Nov 17;387(20):1833–42.

72. Wang LT, Pereira LS, Flores-Garcia Y, O'Connor J, Flynn BJ, Schön A, et al. A Potent Anti-Malarial Human Monoclonal Antibody Targets Circumsporozoite Protein Minor Repeats and Neutralizes Sporozoites in the Liver. Immunity. 2020 Oct 13;53(4):733-744.e8.

73. Corey L, Gilbert PB, Juraska M, Montefiori DC, Morris L, Karuna ST, et al. Two Randomized Trials of Neutralizing Antibodies to Prevent HIV-1 Acquisition. N Engl J Med. 2021 Mar 18;384(11):1003–14.

74. Wu X, Yang ZY, Li Y, Hogerkorp CM, Schief WR, Seaman MS, et al. Rational design of envelope identifies broadly neutralizing human monoclonal antibodies to HIV-1. Science. 2010 Aug 13;329(5993):856–61.

75. Li T, Han X, Gu C, Guo H, Zhang H, Wang Y, et al. Potent SARS-CoV-2 neutralizing antibodies with protective efficacy against newly emerged mutational variants. Nat Commun. 2021 Nov 2;12(1):1–11.

76. Franz B, May KF Jr, Dranoff G, Wucherpfennig K. Ex vivo characterization and isolation of rare memory B cells with antigen tetramers. Blood. 2011 Jul 14;118(2):348–57.

77. Mathew NR, Jayanthan JK, Smirnov IV, Robinson JL, Axelsson H, Nakka SS, et al. Single-cell BCR and transcriptome analysis after influenza infection reveals spatiotemporal dynamics of antigen-specific B cells. Cell Reports. 2021 Jun 22;35(12):109286.

78. Taylor JJ, Pape KA, Jenkins MK. A germinal center–independent pathway generates unswitched memory B cells early in the primary response. J Exp Med. 2012 Feb 27;209(3):597–606.

79. Schwartz MA, Kolhatkar NS, Thouvenel C, Khim S, Rawlings DJ. CD4+ T Cells and CD40 Participate in Selection and Homeostasis of Peripheral B Cells. J Immunol. 2014 Oct 1;193(7):3492–502.

80. Rodda LB, Netland J, Shehata L, Pruner KB, Morawski PA, Thouvenel CD, et al. Functional SARS-CoV-2-Specific Immune Memory Persists after Mild COVID-19. Cell. 2021 Jan 7;184(1):169-183.e17.

81. Rodda LB, Netland J, Shehata L, Pruner KB, Morawski PA, Thouvenel CD, et al. Functional SARS-CoV-2-Specific Immune Memory Persists after Mild COVID-19. Cell. 2021 Jan 7;184(1):169-183.e17.

82. Devito C, Ellegård R, Falkeborn T, Svensson L, Ohlin M, Larsson M, et al. Human IgM monoclonal antibodies block HIV-transmission to immune cells in cervico-vaginal tissues and across polarized epithelial cells in vitro. Sci Rep. 2018 Jul 5;8(1):1–12.

83. Keyt BA, Baliga R, Sinclair AM, Carroll SF, Peterson MS. Structure, Function, and Therapeutic Use of IgM Antibodies. Antibodies. 2020 Dec;9(4):53.

84. Wang Z, Lorenzi JCC, Muecksch F, Finkin S, Viant C, Gaebler C, et al. Enhanced SARS-CoV-2 neutralization by dimeric IgA. Sci Transl Med. 2021 Jan 20;13(577):eabf1555.

85. Dan JM, Mateus J, Kato Y, Hastie KM, Yu ED, Faliti CE, et al. Immunological memory to SARS-CoV-2 assessed for up to 8 months after infection. Science. 2021 Feb 5;371(6529):eabf4063.

86. Casadevall A, Focosi D. SARS-CoV-2 variants resistant to monoclonal antibodies in immunocompromised patients constitute a public health concern. J Clin Invest [Internet]. 2023 Mar 16 [cited 2023 Jun 2];133(6). Available from: https://www.jci.org/articles/view/168603#B1

87. Starr TN, Greaney AJ, Addetia A, Hannon WW, Choudhary MC, Dingens AS, et al. Prospective mapping of viral mutations that escape antibodies used to treat COVID-19. Science. 2021 Feb 19;371(6531):850–4.

88. Focosi D, McConnell S, Casadevall A, Cappello E, Valdiserra G, Tuccori M. Monoclonal antibody therapies against SARS-CoV-2. Lancet Infect Dis. 2022 Nov 1;22(11):e311–26.

89. Gupta A, Konnova A, Smet M, Berkell M, Savoldi A, Morra M, et al. Host immunological responses facilitate development of SARS-CoV-2 mutations in patients receiving monoclonal antibody treatments. J Clin Invest. 2023 Mar 15;133(6):e166032.

90. Planas D, Saunders N, Maes P, Guivel-Benhassine F, Planchais C, Buchrieser J, et al. Considerable escape of SARS-CoV-2 Omicron to antibody neutralization. Nature. 2022 Feb;602(7898):671–5.

91. VanBlargan LA, Errico JM, Halfmann PJ, Zost SJ, Crowe JE, Purcell LA, et al. An infectious SARS-CoV-2 B.1.1.529 Omicron virus escapes neutralization by therapeutic monoclonal antibodies. Nat Med. 2022 Mar;28(3):490–5.

92. Sherchan R, Cannady J. Casirivimab. In: StatPearls [Internet]. Treasure Island (FL): StatPearls Publishing; 2023 [cited 2023 Jun 2]. Available from: http://www.ncbi.nlm.nih.gov/books/NBK572124/

93. Julg B, Stephenson KE, Wagh K, Tan SC, Zash R, Walsh S, et al. Safety and antiviral activity of triple combination broadly neutralizing monoclonal antibody therapy against HIV-1: a phase 1 clinical trial. Nat Med. 2022 Jun;28(6):1288–96.

94. Euler Z, Bunnik EM, Burger JA, Boeser-Nunnink BDM, Grijsen ML, Prins JM, et al. Activity of Broadly Neutralizing Antibodies, Including PG9, PG16, and VRC01, against Recently Transmitted Subtype B HIV-1 Variants from Early and Late in the Epidemic. Journal of Virology. 2011 Jul 15;85(14):7236–45.

95. Bouvin-Pley M, Morgand M, Moreau A, Jestin P, Simonnet C, Tran L, et al. Evidence for a Continuous Drift of the HIV-1 Species towards Higher Resistance to Neutralizing Antibodies over the Course of the Epidemic. PLOS Pathogens. 2013 Jul 4;9(7):e1003477.

96. Mancuso G, Midiri A, Gerace E, Biondo C. Bacterial Antibiotic Resistance: The Most Critical Pathogens. Pathogens. 2021 Oct 12;10(10):1310.

97. Weiner-Lastinger LM, Abner S, Edwards JR, Kallen AJ, Karlsson M, Magill SS, et al. Antimicrobial-resistant pathogens associated with adult healthcare-associated infections: Summary of data reported to the National Healthcare Safety Network, 2015–2017. Infect Control Hosp Epidemiol. 2020 Jan;41(1):1–18.

98. Sato H, Frank D. Multi-Functional Characteristics of the Pseudomonas aeruginosa Type III Needle-Tip Protein, PcrV; Comparison to Orthologs in other Gram-negative Bacteria. Frontiers in Microbiology [Internet]. 2011 [cited 2022 May 30];2. Available from: https://www.frontiersin.org/article/10.3389/fmicb.2011.00142

99. François B, Luyt CE, Dugard A, Wolff M, Diehl JL, Jaber S, et al. Safety and pharmacokinetics of an anti-PcrV PEGylated monoclonal antibody fragment in mechanically ventilated patients colonized with Pseudomonas aeruginosa: A randomized,double-blind, placebo-controlled trial*. Critical Care Medicine. 2012 Aug;40(8):2320–6.

100. Baer M, Sawa T, Flynn P, Luehrsen K, Martinez D, Wiener-Kronish JP, et al. An Engineered Human Antibody Fab Fragment Specific for Pseudomonas aeruginosa PcrV Antigen Has Potent Antibacterial Activity. Infect Immun. 2009 Mar;77(3):1083–90.

101. Warrener P, Varkey R, Bonnell JC, DiGiandomenico A, Camara M, Cook K, et al. A Novel Anti-PcrV Antibody Providing Enhanced Protection against Pseudomonas aeruginosa in Multiple Animal Infection Models. Antimicrob Agents Chemother. 2014 Aug;58(8):4384–91.

102. Chastre J, François B, Bourgeois M, Komnos A, Ferrer R, Rahav G, et al. Safety, efficacy, and pharmacokinetics of gremubamab (MEDI3902), an anti-Pseudomonas aeruginosa bispecific human monoclonal antibody, in P. aeruginosa-colonised, mechanically ventilated intensive care unit patients: a randomised controlled trial. Critical Care. 2022 Nov 15;26(1):355.

103. Hale M, Netland J, Chen Y, Thouvenel CD, Smith KN, Rich LM, et al. IgM antibodies derived from memory B cells are potent cross-variant neutralizers of SARS-CoV-2. J Exp Med. 2022 Sep 5;219(9):e20220849.

104. Mauch RM, Levy CE. Serum antibodies to Pseudomonas aeruginosa in cystic fibrosis as a diagnostic tool: A systematic review. Journal of Cystic Fibrosis. 2014 Sep 1;13(5):499–507.

105. Moss J, Ehrmantraut ME, Banwart BD, Frank DW, Barbieri JT. Sera from Adult Patients with Cystic Fibrosis Contain Antibodies to Pseudomonas aeruginosa Type III Apparatus. Infection and Immunity. 2001 Feb;69(2):1185–8.

106. McConnell MJ. Where are we with monoclonal antibodies for multidrug-resistant infections? Drug Discovery Today. 2019 May 1;24(5):1132–8.

107. Allewelt M, Coleman FT, Grout M, Priebe GP, Pier GB. Acquisition of Expression of the Pseudomonas aeruginosa ExoU Cytotoxin Leads to Increased Bacterial Virulence in a Murine Model of Acute Pneumonia and Systemic Spread. Infect Immun. 2000 Jul;68(7):3998–4004.

108. Rubelt F, Bolen CR, McGuire HM, Vander Heiden JA, Gadala-Maria D, Levin M, et al. Individual heritable differences result in unique cell lymphocyte receptor repertoires of naïve and antigen-experienced cells. Nat Commun. 2016 Mar 23;7:11112.

109. Yaeger LN, Coles VE, Chan DCK, Burrows LL. How to kill Pseudomonas—emerging therapies for a challenging pathogen. Annals of the New York Academy of Sciences. 2021;1496(1):59–81.

110. Moriyama K, Wiener-Kronish JP, Sawa T. Protective effects of affinity-purified antibody and truncated vaccines against Pseudomonas aeruginosa V-antigen in neutropenic mice. Microbiology and Immunology. 2009;53(11):587–94.

111. Goure J, Broz P, Attree O, Cornelis GR, Attree I. Protective Anti-V Antibodies Inhibit Pseudomonas and Yersinia Translocon Assembly within Host Membranes. The Journal of Infectious Diseases. 2005;192(2):218–25.

112. Sawa T, Yahr TL, Ohara M, Kurahashi K, Gropper MA, Wiener-Kronish JP, et al. Active and passive immunization with the Pseudomonas V antigen protects against type III intoxication and lung injury. Nat Med. 1999 Apr;5(4):392–8.

113. Sécher T, Dalonneau E, Ferreira M, Parent C, Azzopardi N, Paintaud G, et al. In a murine model of acute lung infection, airway administration of a therapeutic antibody confers greater protection than parenteral administration. Journal of Controlled Release. 2019 Jun 10;303:24–33.

114. Jain R, Beckett VV, Konstan MW, Accurso FJ, Burns JL, Mayer-Hamblett N, et al. KB001-A, a novel anti-inflammatory, found to be safe and well-tolerated in cystic fibrosis patients infected with Pseudomonas aeruginosa. J Cyst Fibros. 2018 Jul;17(4):484–91.

115. DiGiandomenico A, Warrener P, Hamilton M, Guillard S, Ravn P, Minter R, et al. Identification of broadly protective human antibodies to Pseudomonas aeruginosa exopolysaccharide Psl by phenotypic screening. Journal of Experimental Medicine. 2012 Jun 25;209(7):1273–87.

116. De Tavernier E, Detalle L, Morizzo E, Roobrouck A, De Taeye S, Rieger M, et al. High Throughput Combinatorial Formatting of PcrV Nanobodies for Efficient Potency Improvement. Journal of Biological Chemistry. 2016 Jul;291(29):15243–55.

117. Song L, Cohen D, Ouyang Z, Cao Y, Hu X, Liu XS. TRUST4: immune repertoire reconstruction from bulk and single-cell RNA-seq data. Nat Methods. 2021 Jun;18(6):627–30.

118. Alamyar E, Duroux P, Lefranc MP, Giudicelli V. IMGT(®) tools for the nucleotide analysis of immunoglobulin (IG) and T cell receptor (TR) V-(D)-J repertoires, polymorphisms, and IG mutations: IMGT/V-QUEST and IMGT/HighV-QUEST for NGS. Methods Mol Biol. 2012;882:569–604.

119. Ye J, Ma N, Madden TL, Ostell JM. IgBLAST: an immunoglobulin variable domain sequence analysis tool. Nucleic Acids Res. 2013 Jul;41(Web Server issue):W34-40.

120. Ehrenmann F, Lefranc MP. IMGT/3Dstructure-DB: querying the IMGT database for 3D structures in immunology and immunoinformatics (IG or antibodies, TR, MH, RPI, and FPIA). Cold Spring Harb Protoc. 2011 Jun 1;2011(6):750–61.

121. Matsumoto ML. Molecular Mechanisms of Multimeric Assembly of IgM and IgA. Annu Rev Immunol. 2022 Jan 21;

122. Zhang J, Zhang H, Sun L. Therapeutic antibodies for COVID-19: is a new age of IgM, IgA and bispecific antibodies coming? MAbs. 2022;14(1):2031483.

123. Kreuzberger N, Hirsch C, Chai KL, Tomlinson E, Khosravi Z, Popp M, et al. SARS-CoV-2-neutralising monoclonal antibodies for treatment of COVID-19. Cochrane Database Syst Rev. 2021 Sep 2;9:CD013825.

124. Greaney AJ, Starr TN, Eguia RT, Loes AN, Khan K, Karim F, et al. A SARS-CoV-2 variant elicits an antibody response with a shifted immunodominance hierarchy. PLOS Pathogens. 2022 Feb 8;18(2):e1010248.

125. Harvey WT, Carabelli AM, Jackson B, Gupta RK, Thomson EC, Harrison EM, et al. SARS-CoV-2 variants, spike mutations and immune escape. Nat Rev Microbiol. 2021 Jul;19(7):409–24.

126. Galimidi RP, Klein JS, Politzer MS, Bai S, Seaman MS, Nussenzweig MC, et al. Intra-Spike Crosslinking Overcomes Antibody Evasion by HIV-1. Cell. 2015 Jan 29;160(3):433–46.

127. Tai L, Zhu G, Yang M, Cao L, Xing X, Yin G, et al. Nanometer-resolution in situ structure of the SARS-CoV-2 postfusion spike protein. PNAS. 2021 Nov 30;118(48):e2112703118.

128. Zhang L, Jackson CB, Mou H, Ojha A, Peng H, Quinlan BD, et al. SARS-CoV-2 spike-protein D614G mutation increases virion spike density and infectivity. Nat Commun. 2020 Nov 26;11(1):1–9.

129. Victora GD, Nussenzweig MC. Germinal Centers. Annu Rev Immunol. 2012 Apr 23;30(1):429–57.

130. Lederer K, Bettini E, Parvathaneni K, Painter MM, Agarwal D, Lundgreen KA, et al. Germinal center responses to SARS-CoV-2 mRNA vaccines in healthy and immunocompromised individuals. Cell. 2022 Mar 17;185(6):1008-1024.e15.

131. Zhang Z, Mateus J, Coelho CH, Dan JM, Moderbacher CR, Gálvez RI, et al. Humoral and cellular immune memory to four COVID-19 vaccines [Internet]. bioRxiv; 2022 [cited 2022 Mar 30]. p. 2022.03.18.484953. Available from: https://www.biorxiv.org/content/10.1101/2022.03.18.484953v1

132. Bullen G, Galson JD, Hall G, Villar P, Moreels L, Ledsgaard L, et al. Cross-Reactive SARS-CoV-2 Neutralizing Antibodies From Deep Mining of Early Patient Responses. Front Immunol. 2021;12:678570.

133. Callegari I, Schneider M, Berloffa G, Mühlethaler T, Holdermann S, Galli E, et al. Potent neutralization by monoclonal human IgM against SARS-CoV-2 is impaired by class switch. EMBO Rep. 2022 May 12;e53956.

134. Lenti MV, Aronico N, Pellegrino I, Boveri E, Giuffrida P, Borrelli de Andreis F, et al. Depletion of circulating IgM memory B cells predicts unfavourable outcome in COVID-19. Sci Rep. 2020 Nov 30;10(1):1–9.

135. Newell KL, Clemmer DC, Cox JB, Kayode YI, Zoccoli-Rodriguez V, Taylor HE, et al. Switched and unswitched memory B cells detected during SARS-CoV-2 convalescence correlate with limited symptom duration. PLOS ONE. 2021 Jan 28;16(1):e0244855.

136. Piepenbrink MS, Park JG, Oladunni FS, Deshpande A, Basu M, Sarkar S, et al. Therapeutic activity of an inhaled potent SARS-CoV-2 neutralizing human monoclonal antibody in hamsters. Cell Reports Medicine. 2021 Mar 16;2(3):100218.

137. Purtha WE, Tedder TF, Johnson S, Bhattacharya D, Diamond MS. Memory B cells, but not long-lived plasma cells, possess antigen specificities for viral escape mutants. Journal of Experimental Medicine. 2011 Dec 12;208(13):2599–606.

138. Barnes CO, Jette CA, Abernathy ME, Dam KMA, Esswein SR, Gristick HB, et al. SARS-CoV-2 neutralizing antibody structures inform therapeutic strategies. Nature. 2020 Dec;588(7839):682–7.

139. Pinto D, Park YJ, Beltramello M, Walls AC, Tortorici MA, Bianchi S, et al. Cross-neutralization of SARS-CoV-2 by a human monoclonal SARS-CoV antibody. Nature. 2020 Jul;583(7815):290–5.

140. Yuan M, Wu NC, Zhu X, Lee CCD, So RTY, Lv H, et al. A highly conserved cryptic epitope in the receptor binding domains of SARS-CoV-2 and SARS-CoV. Science. 2020 May 8;368(6491):630–3.

141. Nabel KG, Clark SA, Shankar S, Pan J, Clark LE, Yang P, et al. Structural basis for continued antibody evasion by the SARS-CoV-2 receptor binding domain. Science. 2022 Jan 21;375(6578):eabl6251.

142. Hughey CT, Brewer JW, Colosia AD, Rosse WF, Corley RB. Production of IgM Hexamers by Normal and Autoimmune B Cells: Implications for the Physiologic Role of Hexameric IgM. The Journal of Immunology. 1998 Oct 15;161(8):4091–7.

143. Crawford KHD, Eguia R, Dingens AS, Loes AN, Malone KD, Wolf CR, et al. Protocol and Reagents for Pseudotyping Lentiviral Particles with SARS-CoV-2 Spike Protein for Neutralization Assays. Viruses. 2020 May 6;12(5):513.

144. Ku Z, Xie X, Hinton PR, Liu X, Ye X, Muruato AE, et al. Nasal delivery of an IgM offers broad protection from SARS-CoV-2 variants. Nature. 2021 Jul;595(7869):718–23.

145. Samsudin F, Yi Yeo J, Ken-En Gan S, J. Bond P. Not all therapeutic antibody isotypes are equal: the case of IgM versus IgG in Pertuzumab and Trastuzumab. Chemical Science. 2020;11(10):2843–54.

146. Muller NF, Wagner C, Frazar CD, Roychoudhury P, Lee J, Moncla LH, et al. Viral genomes reveal patterns of the SARS-CoV-2 outbreak in Washington State. Sci Transl Med. 2021 May 26;13(595):eabf0202.

147. Brouwer PJM, Caniels TG, van der Straten K, Snitselaar JL, Aldon Y, Bangaru S, et al. Potent neutralizing antibodies from COVID-19 patients define multiple targets of vulnerability. Science. 2020 Aug 7;369(6504):643–50.

148. Kreer C, Zehner M, Weber T, Ercanoglu MS, Gieselmann L, Rohde C, et al. Longitudinal Isolation of Potent Near-Germline SARS-CoV-2-Neutralizing Antibodies from COVID-19 Patients. Cell. 2020 Aug 20;182(4):843-854.e12.

149. Sakharkar M, Rappazzo CG, Wieland-Alter WF, Hsieh CL, Wrapp D, Esterman ES, et al. Prolonged evolution of the human B cell response to SARS-CoV-2 infection. Science Immunology. 2021 Feb 23;6(56):eabg6916.

150. Ruggiero A, Piubelli C, Calciano L, Accordini S, Valenti MT, Carbonare LD, et al. SARS-CoV-2 vaccination elicits unconventional IgM specific responses in naïve and previously COVID-19-infected individuals. eBioMedicine. 2022 Mar 1;77:103888.

151. Tan CW, Chia WN, Qin X, Liu P, Chen MIC, Tiu C, et al. A SARS-CoV-2 surrogate virus neutralization test based on antibody-mediated blockage of ACE2–spike protein–protein interaction. Nat Biotechnol. 2020 Sep;38(9):1073–8.

152. Clark SA, Clark LE, Pan J, Coscia A, McKay LGA, Shankar S, et al. SARS-CoV-2 evolution in an immunocompromised host reveals shared neutralization escape mechanisms. Cell. 2021 May 13;184(10):2605-2617.e18.

153. Greaney AJ, Starr TN, Barnes CO, Weisblum Y, Schmidt F, Caskey M, et al. Mapping mutations to the SARS-CoV-2 RBD that escape binding by different classes of antibodies. Nat Commun. 2021 Jul 7;12(1):1–14.

154. Planas D, Veyer D, Baidaliuk A, Staropoli I, Guivel-Benhassine F, Rajah MM, et al. Reduced sensitivity of SARS-CoV-2 variant Delta to antibody neutralization. Nature. 2021 Aug;596(7871):276–80.

155. Brewer JW, Randall TD, Parkhouse RM, Corley RB. Mechanism and subcellular localization of secretory IgM polymer assembly. Journal of Biological Chemistry. 1994 Jun 24;269(25):17338–48.

156. Micol R, Kayal S, Mahlaoui N, Beauté J, Brosselin P, Dudoit Y, et al. Protective effect of IgM against colonization of the respiratory tract by nontypeable Haemophilus influenzae in patients with hypogammaglobulinemia. J Allergy Clin Immunol. 2012 Mar 1;129(3):770–7.

157. Altman MC, Reeves SR, Parker AR, Whalen E, Misura KM, Barrow KA, et al. Interferon response to respiratory syncytial virus by bronchial epithelium from children with asthma is inversely correlated with pulmonary function. J Allergy Clin Immunol. 2018 Aug;142(2):451–9.

158. Pisil Y, Yazici Z, Shida H, Miura T. Is SARS-CoV-2 Neutralized More Effectively by IgM and IgA than IgG Having the Same Fab Region? Pathogens. 2021 Jun;10(6):751.

159. Hunt AC, Case JB, Park YJ, Cao L, Wu K, Walls AC, et al. Multivalent designed proteins neutralize SARS-CoV-2 variants of concern and confer protection against infection in mice. Science Translational Medicine. 2022;0(0):eabn1252.

160. Mast FD, Fridy PC, Ketaren NE, Wang J, Jacobs EY, Olivier JP, et al. Highly synergistic combinations of nanobodies that target SARS-CoV-2 and are resistant to escape. Elife. 2021 Dec 7;10:e73027.

161. Rujas E, Kucharska I, Tan YZ, Benlekbir S, Cui H, Zhao T, et al. Multivalency transforms SARS-CoV-2 antibodies into ultrapotent neutralizers. Nat Commun. 2021 Jun 16;12(1):1–12.

162. Xu J, Xu K, Jung S, Conte A, Lieberman J, Muecksch F, et al. Nanobodies from camelid mice and llamas neutralize SARS-CoV-2 variants. Nature. 2021;595(7866):278–82.

163. Matz H, Munir D, Logue J, Dooley H. The immunoglobulins of cartilaginous fishes. Developmental & Comparative Immunology. 2021 Feb 1;115:103873.

164. Arakawa T, Wen J. Determination of Carbohydrate Contents from Excess Light Scattering. Analytical Biochemistry. 2001 Dec 15;299(2):158–61.

165. Moh ESX, Lin CH, Thaysen-Andersen M, Packer NH. Site-Specific N-Glycosylation of Recombinant Pentameric and Hexameric Human IgM. J Am Soc Mass Spectrom. 2016 Jul;27(7):1143–55.

166. Rodda LB, Morawski PA, Pruner KB, Fahning ML, Howard CA, Franko N, et al. Imprinted SARS-CoV-2-specific memory lymphocytes define hybrid immunity. Cell. 2022 Mar 17;

167. Erasmus JH, Khandhar AP, O'Connor MA, Walls AC, Hemann EA, Murapa P, et al. An Alphavirus-derived replicon RNA vaccine induces SARS-CoV-2 neutralizing antibody and T cell responses in mice and nonhuman primates. Science Translational Medicine. 2020 Aug 5;12(555):eabc9396.

168. Wu W, Badrane H, Arora S, Baker HV, Jin S. MucA-mediated coordination of type III secretion and alginate synthesis in Pseudomonas aeruginosa. J Bacteriol. 2004 Nov;186(22):7575–85.

169. Jain M, Ramirez D, Seshadri R, Cullina JF, Powers CA, Schulert GS, et al. Type III Secretion Phenotypes of Pseudomonas aeruginosa Strains Change during Infection of Individuals with Cystic Fibrosis. J Clin Microbiol. 2004 Nov;42(11):5229–37.

170. Conrey PE, Denu L, O'Boyle KC, Rozich I, Green J, Maslanka J, et al. IgA deficiency destabilizes homeostasis toward intestinal microbes and increases systemic immune dysregulation. Science Immunology. 2023 May 26;8(83):eade2335.

171. Fadlallah J, El Kafsi H, Sterlin D, Juste C, Parizot C, Dorgham K, et al. Microbial ecology perturbation in human IgA deficiency. Sci Transl Med. 2018 May 2;10(439):eaan1217.

172. Mella MA, Lavrinienko A, Akhi R, Hindström R, Nissinen AE, Wang C, et al. Compensatory IgM to the Rescue: Patients with Selective IgA Deficiency Have Increased Natural IgM Antibodies to MAA-LDL and No Changes in Oral Microbiota. Immunohorizons. 2021 Apr 23;5(4):170–81.

173. Klunk J, Vilgalys TP, Demeure CE, Cheng X, Shiratori M, Madej J, et al. Evolution of immune genes is associated with the Black Death. Nature. 2022 Nov;611(7935):312–9.

174. Andrades Valtueña A, Neumann GU, Spyrou MA, Musralina L, Aron F, Beisenov A, et al. Stone Age Yersinia pestis genomes shed light on the early evolution, diversity, and ecology of plague. Proc Natl Acad Sci U S A. 2022 Apr 26;119(17):e2116722119.

175. Gessard C. On the Blue and Green Coloration that Appears on Bandages. Reviews of Infectious Diseases. 1984 Sep 1;6(Supplement_3):S775–6.

176. Elusys Therapeutics. Elusys Receives Second Delivery Order From U.S. Government for ANTHIM®, its Treatment for Inhalation Anthrax [Internet]. 2018 [cited 2023 Jun 9]. Available from: https://www.prnewswire.com/news-releases/elusys-receives-second-delivery-order-from-us-government-for-anthim-its-treatment-for-inhalation-anthrax-300634114.html

177. Strout V. Monoclonal Antibody for Treatment of Inhalation Anthrax (NIH 1UC1AI062546) [Internet]. Grantome. 2004 [cited 2023 Jun 9]. Available from: https://grantome.com/grant/NIH/UC1-AI062546-01

178. Hao L, Hsiang TY, Dalmat RR, Ireton R, Morton JF, Stokes C, et al. Dynamics of SARS-CoV-2 VOC Neutralization and Novel mAb Reveal Protection against Omicron. Viruses. 2023 Feb 14;15(2):530.

179. Singh T, Hwang KK, Miller AS, Jones RL, Lopez CA, Dulson SJ, et al. A Zika virus-specific IgM elicited in pregnancy exhibits ultrapotent neutralization. Cell. 2022 Dec 8;185(25):4826-4840.e17.

180. Baliga R, Ng D, Key B. IgM Fc and J-chain mutations that affect IgM serum half-life.

181. Hung KL, Meitlis I, Hale M, Chen CY, Singh S, Jackson SW, et al. Engineering Protein-Secreting Plasma Cells by Homology-Directed Repair in Primary Human B Cells. Mol Ther. 2018 Feb 7;26(2):456–67.

182. Cheng RYH, Hung KL, Zhang T, Stoffers CM, Ott AR, Suchland ER, et al. Ex vivo engineered human plasma cells exhibit robust protein secretion and long-term engraftment in vivo. Nat Commun. 2022 Oct 16;13(1):6110.